Università degli Studi di Milano

Scuola di Dottorato in Medicina Molecolare

Curriculum in Medicina Molecolare delle Reazioni Immuni ed Infiammatorie

CICLO XXVII

Anno Accademico 2013/2014

TESI DI DOTTORATO DI RICERCA

Anti-Tumoral Effects of miR-3189-3p in Glioblastoma

Settore MED/04 - Patologia Generale

TESI DI: Dott.ssa Mariacristina De Luca
MATRICOLA: R09568

TUTORE: Prof.ssa Daria Trabattoni
CO-TUTORE: Prof.ssa Francesca Peruzzi
COORDINATORE: Chiar.mo Prof. Mario Clerici

RIASSUNTO

Introduzione: *Il glioblastoma e' un tumore maligno del cervello, della categoria dei gliomi, caratterizzato da rapida crescita cellulare, elevata invasivita', aggressivita' e resistenza alla radio e chemioterapia. I soggetti colpiti da questa forma tumorale, che costituisce circa il 50% delle neoplasie maligne cerebrali negli adulti, hanno in media un'aspettativa di vita di quindici mesi. Il trattamento di base prevede l'asportazione della massa tumorale in combinazione alla radioterapia, eventualmente seguite da chemioterapia con temozolomide. Data l'estrema necessita' di sviluppare nuove strategie terapeutiche per questo tumore fino ad ora praticamente incurabile, l'individuazione dei meccanismi molecolari che sono alla base della proliferazione e della sopravvivenza del glioblastoma e' di fondamentale importanza.*

Growth Differentiation Factor 15 (GDF15), conosciuto anche con il nome di Nonsteroidal Anti-Inflammatory drug-activated Gene-1 (NAG-1) o Macrophage Inhibitory Cytokine-1 (MIC-1) e' una proteina della famiglia del transforming growth factor-β (TGF-β). Il gene che codifica per GDF15 e' costituito da due esoni che generano un precursore composto da un pro-peptide di 167 amminoacidi e da un dominio corrispondente al peptide maturo di 112 amminoacidi. In seguito alla dimerizzazione, avviene il clivaggio del precursore con il successivo rilascio del peptide maturo di 112 amminoacidi nella matrice extracellulare, dove agisce come dimero biologicamente attivo. L'espressione di GDF15 nei tessuti e' notevolmente indotta in risposta a stimolazione con differenti farmaci anti-infiammatori, agenti citotossici, agonisti dei recettori della famiglia dei peroxisome proliferator-activated receptors (PPAR) e farmaci antitumorali.

Il ruolo di GDF15 nella tumorigenesi non e' stato ancora del tutto chiarito. Evidenze sperimentali dimostrano che elevati livelli di trascritto sono presenti in pazienti durante la progressione dello stadio tumorale da astrocitoma a glioblastoma, ma altri studi hanno dimostrato come l'espressione di GDF15 sia indotta in risposta a trattamenti chemioterapici.

Metodi: *L'espressione di GDF15 mediante saggi di Real-time PCR, Western Blot ed Elisa e del miR-3189-3p mediante Real-time PCR e' stata valutata nella linea cellulare di glioblastoma LN-229 in seguito a stimolazione con Fenofibrato. Saggi di transfezione in vitro sono stati effettuati allo scopo di validare il targeting del miR-3189-3p sulla regione 3'UTR dei due geni SF3B2 e p63RhoGEF. Analisi di Real-time PCR, Western Blot, di proliferazione e migrazione cellulare in vitro e l'iniezione subcutanea ed intracranica in topi nudi di cellule di glioblastoma precedentemente transfettate con il miR-3189-3p, sono state eseguite al fine di studiare il ruolo funzionale del miR-3189-3p.*

Risultati: *Risultati precedentemente ottenuti nel nostro laboratorio hanno dimostrato che la stimolazione della linea cellulare LN-229 con il fenofibrato, un agonista di PPARα, determina un aumento di espressione di GDF15.*

Nel presente studio, dall'analisi della sequenza genica di GDF15 e' risultata di particolare interesse la presenza di un microRNA, miR-3189, all'interno del suo unico introne, in posizione prossimale all'esone 1. Il pre-mir-3189 contiene due sequenze di microRNA mature all'interno dell sua struttura a forcina: miR-3189-3p e miR-3189-5p, rispettivamente di 21 e 25 nucleotidi. Ad oggi non ci sono studi che abbiano riportato la funzione biologica di tale microRNA, pertanto dato il ruolo che

ricoprono i microRNA nella regolazione genica, scopo principale di questo lavoro e' stato innanzitutto quello di definire gli effetti dei due microRNA, miR-3189-3p e -5p, nella funzione biologica di GDF15 nei glioblastomi.

Abbiamo scoperto che l'induzione del trascritto e della proteina in seguito a stimolazione con fenofibrato e' accompagnata da una elevata espressione del miR-3189-3p e precede gli eventi di apoptosi innescati dal fenofibrato. Nelle medesime condizioni sperimentali non e' stata osservata invece induzione del miR-3189-5p. Inoltre, mediante saggi di transfezione, abbiamo dimostrato che l'espressione ectopica del miR-3189-3p determina una inibizione della proliferazione e della migrazione cellulare mediante il silenziamento di due dei suoi mRNA bersaglio predetti, rispettivamente il fattore di splicing SF3B2 e il fattore di scambio del nucleotide guanina p63RhoGEF.

Dall'analisi di espressione genica su campioni di glioblastoma e di tessuti normali abbiamo trovato che ad un aumento dei livelli di espressione di GDF15 nei glioblastomi corrisponde un decremento dei livelli di miR-3189-3p e, in aggiunta, queste differenze di espressione correlano con un incremento nei livelli di SF3B2 e una tendenza all'aumento in p63RhoGEF.

Infine, esperimenti di iniezione subcutanea e intracranica di cellule di glioblastoma precedentemente transfettate con il miR-3189-3p, hanno mostrato una inibizione della crescita tumorale rispetto a cellule di controllo.

Conclusioni: *Tutte queste evidenze sperimentali supportano e validano il ruolo di miR-3189-3p come oncosoppressore nei glioblastomi mediante il controllo della crescita e della migrazione cellulare attraverso il silenziamento rispettivamente di SF3B2 e p63RhoGEF.*

SUMMARY

Background: *Glioblastoma is a deadly cancer characterized by rapid cell proliferation, high invasiveness, and resistance to radio- and chemotherapy. Patients with this aggressive tumor, which accounts for nearly 50% of all adult brain tumors, have a median survival of approximately 15 months. The standard treatment for glioblastoma involves invasive surgery and radiotherapy, which is often followed by chemotherapy with temolozomide. As the development of novel therapeutic treatments for glioblastoma are desperately needed, it is essential to understand the molecular mechanisms supporting growth and survival of this highly malignant and practically incurable brain tumor.*

Growth Differentiation Factor 15, GDF15, also known as Nonsteroidal Anti-inflammatory drug-activated Gene -1 (NAG-1) or Macrophage Inhibitory Cytokine-1 (MIC-1), is a member of the transforming growth factor-β (TGF-β) superfamily. The GDF15 gene is encoded by two exons to generate a precursor protein containing a 167 amino acid pro-peptide sequence and a 112 amino acid mature domain. Upon dimerization, this precursor protein is cleaved resulting in the release of the 112 amino acid mature GDF15 peptide, which is secreted into the extracellular matrix as a biologically active dimer. GDF15 can be induced by anti-inflammatory drugs, cytotoxic agents, peroxisome proliferator-activated receptor (PPAR) agonist, and anticancer drugs. Increased GDF15 mRNA expression has been reported in patients during malignant progression to glioblastoma, and others have reported that expression levels of GDF15 are upregulated in glioblastoma cells in response to cytotoxic stimuli during chemotherapy treatment. We have previously reported increased expression of GDF15 in the LN-229 glioblastoma cell line following the treatment with fenofibrate, an agonist of PPARα. In this study, we have analyzed the genomic sequence of GDF15 and found it contains a microRNA, miR-3189, encoded within its single intron at a position proximal to exon 1. The precursor sequence encoded by miR-3189 contains two mature microRNA sequences within the stem-loop: miR-3189-3p and miR-3189-5p, of 21 and 25 nucleotides in length, respectively. The biological function of this microRNA has never been described before. Because of the role of microRNAs in gene regulation, we wanted to define the effects of these co-expressed microRNAs, miR-3189-3p and miR-3189-5p, in the biological function of GDF15.

Methods: *The expression of GDF15 by Real-time PCR, Western Blots and Elisa assays and miR-3189-3p by Real-time PCR was evaluated in LN-229 cells stimulated with Fenofibrate. Transfections were performed in order to validate the targeting of miR-3189-3p on the 3'UTR of two of its major predicted targets SF3B2 and p63RhoGEF. The functional role of miR-3189-3p was assessed through Real-time PCR, Western Blot, cell-growth and migration assays, and through both the subcutaneous and the intracranial injection in nude mice.*

Results: *We found that treatment of glioblastoma cells with fenofibrate resulted in a striking increase in GDF15 mRNA and protein levels, which was accompanied by high expression of miR-3189-3p, and preceded fenofibrate-induced apoptosis. In this experimental condition, miR-3189-5p was not detected. Ectopic expression of miR-3189-3p inhibited LN-229 cell growth and migration through downregulation of the splicing factor SF3B2 and the guanine nucleotide exchange factor p63RhoGEF, respectively. In comparison to the normal brain tissue, we also found that glioblastoma clinical samples have increased levels of GDF15 and decreased levels*

of miR-3189-3p, and that these changes correlated with increased expression of SF3B2 and a trend of increased levels for p63RhoGEF. Finally, both the subcutaneous and the intracranial growth of glioblastoma cells expressing miR-3189-3p were significantly reduced when compared to control cells, thus further validating the role of this microRNA as a tumor suppressor.

Conclusions: *Our studies have demonstrated that miR-3189-3p has a tumor-suppressive role by controlling the growth and the migration of glioblastoma cells by targeting the SF3B2 and p63RhoGEF mRNAs.*

TABLE OF CONTENTS

LIST OF ABBREVIATIONS

NcRNA: Non-coding RNA
LncRNA: Long non-coding RNA
SiRNA: Small interfering RNA
PiRNA: Piwi-interacting RNA
SnRNA: Small nuclear RNA
SnoRNA: Small nucleolar RNA
3' UTR: 3' Untraslated Region
5' UTR: 5' Untraslated Region
Pol II: RNA Polymerase II
DGCR8: DiGeorge syndrome Critical Region 8
Exp 5: Exportin 5
Ran: Ras-related Nuclear protein
Ago: Argonaute
Ago2: Argonaute 2
RISC: RNA-Induced Silencing Complex
MiRISC: MicroRNA-Induced Silencing Complex
MiRNP: Micro-RNP, MicroRNA Ribonucleoprotein Complex
TRBP: TAR RNA-Binding Protein
LDBR: Lariat Debranching Enzyme
CDS: Coding Sequence
Dcp1: mRNA Decapping enzyme 1
Dcp2: mRNA Decapping enzyme 2
PB: P-body, Processing Body
PABP: Poly (A)-Binding Protein
MYC: V-Myc Avian Myelocytomatosis Viral Oncogene Homolog
ZEB 1: Zinc Finger E-Box binding Homeobox 1
ZEB 2: Zinc Finger E-Box binding Homeobox 2
MYOD: Myoblast Determination Protein 1
GSK3β: Glycogen Syntetase Kinase 3β
HNRNPA1: Heterogeneous Nuclear Ribonucleoprotein A1
KSRP: KH-type Spicing Regulatory Protein
SNP: Single Nucleotide Polymorphism
TUT4: Terminal Uridylyl Transferase 4
BCDIN3D: Pre-MicroRNA 5' Monophosphate Methyltransferase
XRN1: 5' – 3' exoribonuclease 1
XRN2: 5' – 3' exoribonuclease 2
RRP41: Ribosomal RNA-processing Protein 41
PNPase^{old35}: Polynucleotide Phosphorylase
NGS: Next Generation Sequencing
GBM: Glioblastoma Multiforme
TMZ: Temozolomide
oncomiR: oncogenic microRNA

CDK: Cyclin-dependent Kinase
PTPμ: Protein tyrosin phosphatase μ
giNSC: glioma-initiating neural stem cell
PDGFRα: Platelet-derived Growth Factor Receptor alpha
GDF15: Growth Differentiation Factor 15
TGFβ: Transforming Growth Factor β
NAG-1: Non-steroidal Anti-inflammatory drug-activated Gene 1
MIC-1: Macrophage Inhibitory Cytokine 1
PDF: Prostate-Derived Factor
PTGFβ: Placental TGFβ
PLAB: Placental Bone Morphogenetic Protein
CSF: Cerebrospinal Fluid
SMAD: Small Mother Against Decapentaplegic
NSAIDs: Non-Steroidal Anti-Inflammatory Drugs
Egr-1: Early Growth Response protein 1
NF-kB: Nuclear Factor kappa-light-chain-enhancer of activated B cells
PARP1: Poly (ADP-ribose) Polymerase 1
Calu-15: Calumenin-15
PPARα: Peroxisome Proliferator Receptor α
CPT-1: Carnitine Palmitoyl Transferase 1
FFA: Free Fatty Acid
PDH: Pyruvate Dehydrogenase
RXR: Retinoic Acid Receptor
RE: Responsive Element
PPRE: Peroxisome Poliferator Response Element
VEGF: Vascular Endothelial Growth Factor
IGF-I: Insuline-like Growth Factor 1
FOXO3A: Forkhead-box O Transcription Factor 3A
Bim: BCL2 Like 11
SF3B2: Splicing Factor 3B, subunit 2
p63RhoGEF: Rho Guanine Nucleotide Exchange Factor
SAP: Splicing-assocaited Protein
GPCR: G-protein-coupled Receptor
RIP: RNA-binding protein Immunoprecipitation

INTRODUCTION

1. NON-CODING RNAs

One of the most important advances in the field of contemporary molecular biology has been the discovery of non-coding RNAs (ncRNAs) as molecules with biological relevant role. NcRNAs represent only a small fraction of the genome of prokaryotes, which is generally characterized by protein-coding sequence accounting for 80-95% of it. The proportion of protein-coding genes declines with the simultaneous complexity of the organisms, with a concomitant increase of the number of non-coding intergenic and intronic sequences, most of which are in fact transcribed. Therefore, there seems to exist a progressive shift in transcriptional output between microorganisms and multicellular organisms from mainly protein-coding mRNAs to mainly non-coding RNAs [1,2]. Indeed, according to the International Human Genome Sequencing Consortium, the number of the protein-coding genes encoded by the human genome corresponds to a range of 20.000 – 25.000 and represents only 2% of the genome [3]. Conversely a bigger portion of the human genome (98%), previously considered not functional and named as “junk DNA”, originates thousands of RNA transcripts classified as non-coding RNAs (ncRNAs) [4]. Three major classes of ncRNAs have been determined on the basis of their transcript size: small (~18-31 nucleotides, nt), medium (~31-200 nt) and long non-coding RNAs (lncRNAs, from 200 nt up to several hundred kilobases, kb). The group of small ncRNAs contains small interfering RNAs (siRNAs), microRNAs (miRNAs, miRs) and Piwi interacting RNAs (piRNAs), while medium ncRNAs mainly include small nuclear RNAs (snRNAs) and small nucleolar RNAs (snoRNAs). Very little is known so far about the lncRNA species, which are included in this novel class of non-coding RNAs.

NcRNAs can be further divided into housekeeping ncRNAs such as ribosomal RNAs, transfer RNAs, snRNAs and snoRNAs having crucial roles in many cellular processes and regulatory RNAs such as microRNAs,

siRNAs, piRNAs and lncRNAs that play an important role as epigenetic regulators of gene expression [5]. All of these ncRNAs contribute to the eukaryotic complexity and play a central role in regulating cellular activities.

1.1 MicroRNAs

The discovery of microRNAs can be dated in 1993 with the identification in *Caenorhabditis elegans* of the *lin-4* microRNA gene by Victor Ambros and colleagues [6,7]. The authors found that *lin-4* functions as post-transcriptional regulator of the timing of larval development by inhibiting the expression of its target mRNA *lin-14* by partially base-pairing to sequences located in the mRNA 3' untranslated regions (3'UTRs) [8]. Since that discovery microRNAs have been identified in plant and animal species [9]. In fact, according to the latest version of the microRNA database (miRBase, www.miRbase.org), issued in August 2012, 2042 and 1281 mature microRNAs are respectively cataloged in humans and in mice [10].

MicroRNAs are post-transcriptional regulators of gene expression that function by inhibiting translation of mRNAs [11]. They are endogenously encoded single stranded RNAs of 18-22 nucleotides in length that inhibit mRNA translation through imperfect base-pairing with sequences, which are generally located in the 3'UTR of mRNA transcript [12].

1.1.1 MicroRNA genomic organization

Most microRNA genes are located in the intergenic regions of the genome [13], implying that they are transcribed independently from other adjacent genes. These microRNAs can be organized as monocistronic and possess their own promoter, or polycistronic (clustered), with a shared promoter.

MicroRNAs are also found in the introns of annotated genes, both protein-coding and non-coding. Similarly to the intergenic ones, also these microRNAs can be present as monocistronic or polycistronic and their expression is strictly linked to the transcription of the gene from which they originate.
Some microRNAs derive from spliced-out introns that are essentially equivalent to the pre-microRNAs, and they are therefore called mirtrons. There are also few examples of exonic microRNAs. They often overlap an exon and an intron of a non-coding gene and their maturation often excludes host gene function [14] (***Fig. 1***).

1.1.2 MicroRNA classification and nomenclature

Classification rules for microRNAs have not been precisely identified so far. MicroRNAs that possess identical sequences at nucleotides 2-8 of the mature form generally belong to the same "microRNA family", for example the let-7 family, composed of 14 paralogs loci (microRNA sisters) [15].

The nomenclature of microRNA genes is in part contradictory. Genes encoding paralogs microRNAs are indicated with lettered suffixes (for instance mir-125a and mir-125b). If multiple loci generate the same mature microRNA, numeric suffixes are added at the end of the names of the microRNA loci (for example, mir-125b-1 and mir-125b-2). Furthermore, each locus produces two microRNAs: one from the 5' strand and one from the 3' strand of the precursor, designed as -5p and -3p respectively (for example, miR-125a-5p and miR-125a-3p) [16]. Finally, the mature sequences are generally designated "miR", whereas the precursor hairpins are labelled "mir" [17].

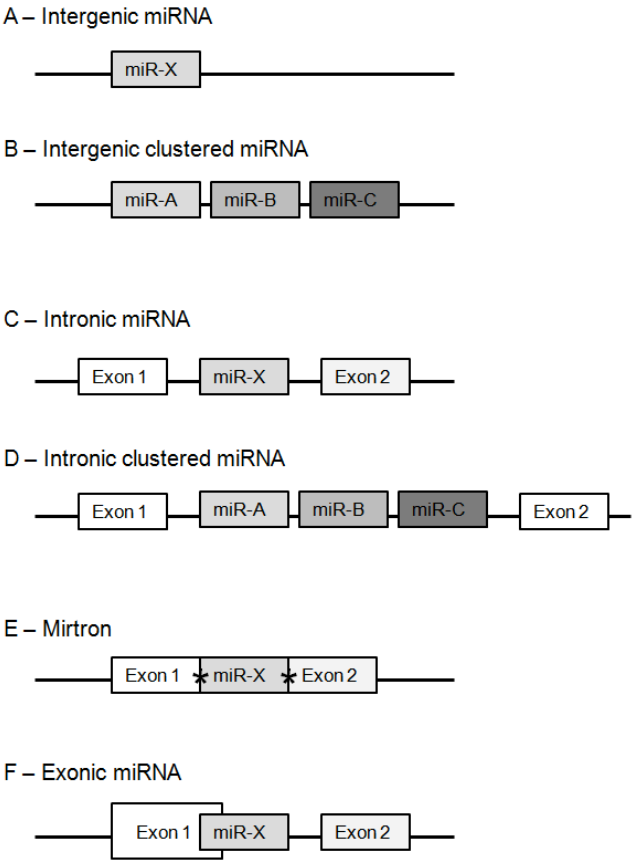

Fig. 1: Genomic organization of microRNAs
Intergenic microRNAs are found in genomic regions distinct from known transcription units. These microRNAs can be monocistronic (A), or polycistronic (B) where several microRNAs are transcribed as cluster of primary transcripts.
Intronic microRNAs are found in the introns of annotated genes, both protein coding and non-coding. These microRNAs can be present as a single microRNA (C) or as a cluster of several microRNAs (D). Intronic microRNAs are thought to be transcribed from the same promoter of their host genes and processed from the introns of host gene trancripts. In the special case of mirtrons (E), the intron is the exact sequence of the pre-microRNA with splice sites on either side (denote by black asterisks). In this case, the Microprocessor complex is thought to be unnecessary in mirtron maturation. Exonic microRNAs are far rarer than either of the types mentioned above and often overlap an exon and an intron of a non-coding gene. These microRNAs are also thought to be transcribed by their host gene promoter and their maturation often excludes host gene function. [Adapted from Olena, 2009, Journal of Cellular Physiology].

1.1.3 Biogenesis of canonical microRNAs

1.1.3.1 Nuclear processing

Except for the class of mirtrons, some viral microRNAs and endogenous tRNA-derived microRNAs [18], microRNA genes are transcribed from non-coding regions of the genome by RNA polymerase II (RNA pol II) into a long primary transcript (pri-microRNAs) [19]. Pri-microRNAs contain a 5' m^7 G capping structure and 3' poly (A) tails, typical properties of class II genes transcripts [19]. Pri-microRNAs can be several kbs long and they can contain one or more stem-loop structures [20]. Those microRNA precursors are subsequently trimmed at the base of the stem-loop by a microprocessor which consists of the nuclear Ribonuclease III, Drosha, and the double-stranded RNA-binding domain protein DGCR8 (DiGeorge syndrome critical region protein 8) into a shorter microRNA stem loop (pre-microRNA) of approximately 60-70 nucleotides in length [21].

1.1.3.2 Nuclear export

Pre-microRNAs are recognized by a member of the karyopherin family of nucleocytoplasmic transport factors Exportin 5 (Exp5) which, not only serves as the nuclear export factor for the pre-microRNAs but also protects the latter from digestion by nucleases [22]. By the cooperative binding to its cargo and to the GTP-bound form of the cofactor Ran (Ras-related Nuclear Protein), Ran-GTP, Exp5 transports pre-microRNAs through the nuclear pores into the cytoplasm [23]. Fundamental requirement for pre-microRNA recognition by Exp5 is the presence of a >14-nt stem region along with a short 3' overhang (1-8 nt) [24].

This pre-microRNA/Exp5/Ran-GTP complex then migrates to the cytoplasm where hydrolysis of Ran-GTP to Ran-GDP induces release of the pre-microRNA cargo.

Once in the cytoplasm, pre-microRNAs are further processed by another Ribonuclease III family member, Dicer, into a ~22 nt long microRNA duplexes, with short 3' overhangs, consisting of a guide strand and a passenger strand.

1.1.3.3 Strand selection

MicroRNA duplexes associate with Argonaute proteins (Ago), the components of the RNA-induced silencing complex (RISC) directly bound to mature microRNAs [25].

One of the two strands of the duplex remains incorporated as mature microRNA into the miRISC complex. At the beginning of the discovery of the microRNAs, it was assessed that the guide strand usually remains incorporated into the miRISC, while the passenger strand (named as microRNA*) is generally degraded [9], but increasing evidence suggests that also the passenger strand can be actively incorporated into the miRISC and works as well. Therefore the nomenclature "passenger strand" or "microRNA*" is not very accurate, while it seems more correct to use the 5p – 3p names for the two strands of the microRNA duplex, since that does not assume that one strand is more important than the other. Indeed, both strands are detected and are equally abundant in some tissues and they can be functional in the same way [26]. Conversely, in other tissues or under certain experimental conditions, there is a strong preference for one of the two strands via a tightly controlled mechanism that has critical biological implications. While the exact mechanisms involved in strand selection are still unclear, it has been hypothesized a role for the relative thermodynamic stability of the 5' ends of the microRNA duplex. The strand with more unstable base pairs at its 5' end is retained into the miRISC [27].

1.1.3.4 MicroRNA assembly into microribonucleoproteins

Following the processing, microRNAs are assembled into ribonucleoprotein (RNP) complexes named micro-RNPs (miRNPs) or microRNA-induced silencing complexes (miRISCs).

The microRNA/RISC (miRISC) complex is composed of several proteins including Dicer, transactivation response RNA-binding protein (TRBP), protein activator of the interferon (PACT) and Argonaute (Ago) [28]. All these proteins were shown to participate in strand selection [29], but the "core" component of miRISC complex is Ago protein-family. In mammalian cells four different paralogs of Ago have been identified: Ago1-4. All of these paralogs can bind endogenous microRNAs, but only Ago2 is characterized by endonuclease activity to cleave complementary target mRNA sequences [30]. Once a microRNA is incorporated into the miRISC, the 2 – 8 nucleotides of the microRNA composing the seed sequence are presented and direct Ago protein to target mRNAs. The consequent binding of microRNAs to the 3' UTR region of mRNAs through an imperfect complementarity leads to mRNA degradation or translational inhibition [15]. Refer to ***Fig. 2*** for a detailed overview of the multi-steps biogenesis of microRNAs.

A - Biogenesis of canonical microRNA

B – Canonical intronic microRNA

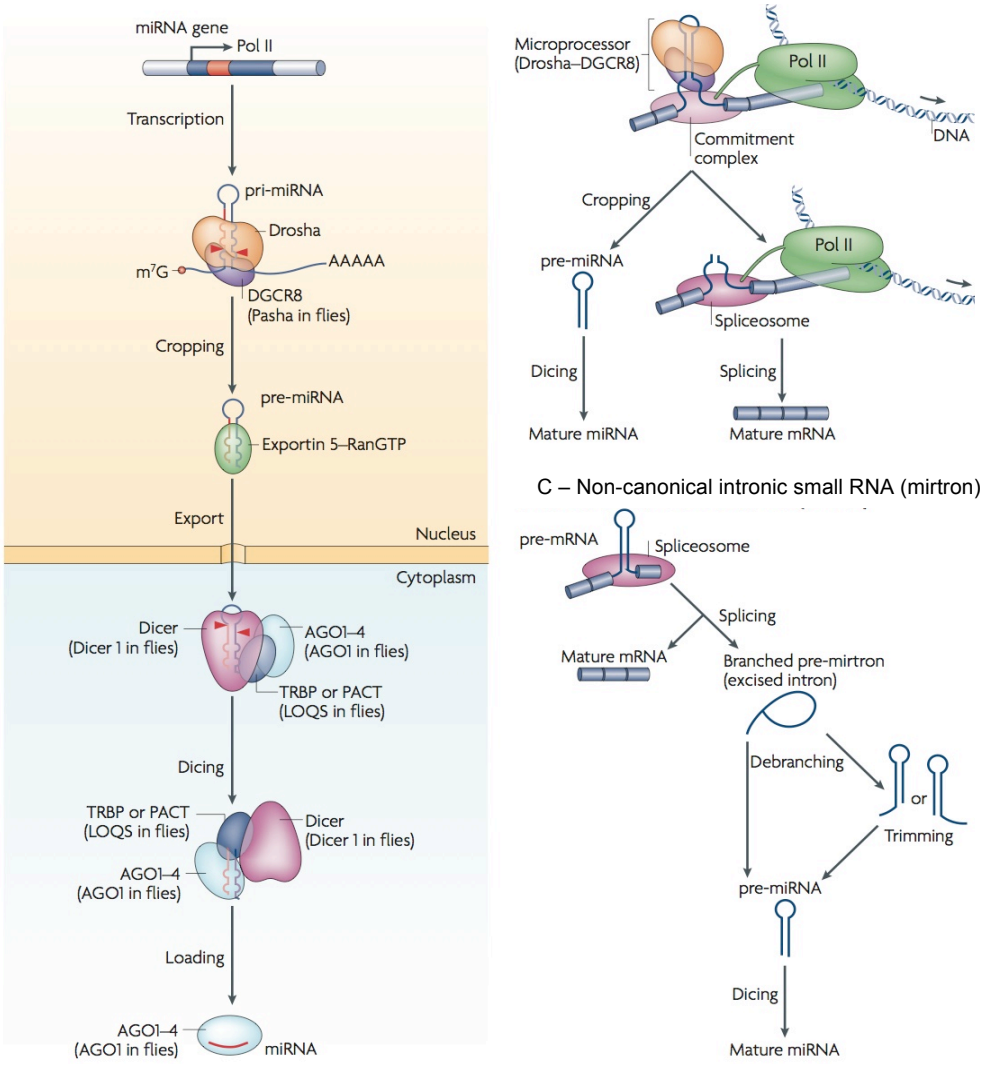

C – Non-canonical intronic small RNA (mirtron)

Fig. 2: Schematic model of canonical and non-canonical microRNA biogenesis pathways.

A - *In the canonical pathways, RNA polymerase II (pol II) transcribed pri-microRNAs are processed in the nucleus by the Drosha–DiGeorge syndrome critical region gene 8 (DGCR8; Pasha in Drosophila melanogaster and Caenorhabditis elegans) complex (also known as the Microprocessor complex) that generates ~65 nt pre-microRNAs, a process named as "cropping". Pre-microRNAs are then recognized and transported into the cytoplasm by the nuclear export factor exportin 5 (EXP5).*

The second step of microRNA processing takes place in the cytoplasm and it is mediate by Dicer, which catalyzes the process named as "dicing" producing microRNA duplexes.
Dicer, TRBP (TAR RNA-binding protein; also known as TARBP2) or PACT (also known as PRKRA), and Argonaute (AGO) 1–4 (also known as EIF2C1–4) mediate the processing of pre-microRNA and the assembly of the RISC (RNA-induced silencing complex) in humans.
***B -** Canonical intronic microRNAs are processed co-transcriptionally before splicing. They require the Microprocessor complex to be generated. The microRNA-containing introns are spliced more slowly than the adjacent introns for unknown reasons. The splicing commitment complex is thought to tether the introns while Drosha cleaves the microRNA hairpin. The pre-microRNA enters the microRNA pathway, whereas the rest of the transcript undergoes pre-mRNA splicing and produces mature mRNA for protein synthesis.*
***C -** Non-canonical intronic small RNAs are produced from spliced introns and debranching. Because such small RNAs (called mirtrons) can derive from small introns whose sequences resemble pre-microRNAs, they bypass the Drosha-processing step. Some introns have tails at either the 5′ end or 3′ end, which will be trimmed before pre-microRNA export. [Adapted from Kim VN, 2009, Biogenesis of small RNAs in animals, Nat Rev].*

1.1.4 Alternative pathways of biogenesis of non-canonical microRNAs

1.1.4.1 The Mirtron pathway

The most noticeable Drosha-independent microRNA biogenesis mechanism is the mirtron pathway, first described in *Drosophila melanogaster* and in *Caenorhabditis elegans* [31]. Mirtrons are usually localized in short introns where the whole intron is equivalent to the pre-microRNA form (***Fig. 2C***). Therefore the first step of mirtrons processing is different from the canonical pathway because the pre-microRNA is cleaved out from the primary transcript by the splicing machinery bypassing the Microprocessor activity [32]. The spliced intron is not linear, but instead it is a lariat in which the 3' branchpoint site is ligated to the 5' end of the intron. After the resolution of this structure by lariat debranching enzyme (LDBR), the intron assumes the pre-microRNA folding and it can enters the "canonical pathway" at this stage, being transferred into the cytoplasm by

Exp5, cleaved by Dicer and loaded into the RISC complex for target regulation [32].

In addition to the originally described type of mirtrons, there are two closely related groups of mirtrons: the 3' – and the 5' – tailed mirtrons. Both of them have the intronic splicing donor and acceptor sites, but they are characterized by extended 3' or 5' single-stranded RNA tails in the pre-microRNA form that are further trimmed by exonucleases before Dicer processing [33,34]. Interestingly, no 3' tailed mirtrons have been identified so far in vertebrate species. Conversely, a number of 5' tailed mirtrons have been found in chicken and various mammals [18,35,36].

1.1.4.2 Dicer-independent processing of microRNAs

Dicer has been viewed as a central processing enzyme in the maturation of small RNAs [37], but recently functional microRNAs that are able to bypass Dicer activity have been discovered. For instance, processing of the pre-miR-451 has been shown to occur by Ago2 slicer catalytic activity instead of Dicer-dependent cleavage [38]. The major determinants that allow this alternative pathway to take place are: the presence of a short 17 bp stem and a 4 nt loop of miR-451 [38,39]. According to the current model, Ago2 binds the microRNA and cleaves the paired passenger strand 10 nt away from the 5' end of the Ago2 bound microRNA guide strand [40]. Importantly, this discovery assigned a novel function of Ago2 protein during the processing step of microRNAs. Indeed, Ago2 possesses not only the cleavage capability of the complementary mRNA targets, but also the slicer activity on pre-microRNAs for the generation of functional mature microRNAs [40].

1.1.5 Mechanisms of microRNA-mediated post-transcriptional gene regulation

The specific sequence for mRNA targets recognition is determined by nucleotides 2 to 8 of the 5' region on the guide microRNA strand. It is usually referred as the "seed sequence" and it is essential for the selection of target messenger RNAs [25]. It is well known that microRNAs recognize and bind complementary sequences usually located in the 3'UTR of mRNA targets, but recent discoveries have shown the presence of non-canonical sites both in the 5'UTR and in the coding sequence (CDS) of mRNAs [41]. The interaction between the seed sequence and the targets results in mRNA degradation or translational inhibition on the basis of a perfect or an imperfect complementarity. Indeed the presence of a perfect complementarity leads to mRNA strand cleavage catalyzed by Ago protein.

Conversely an imperfect base-pairing caused by the presence of mismatches and bulges excludes cleavage and promotes mRNA translational repression [37].

Until today the mechanisms involved in microRNA-mediated repression remain elusive. A number of studies have described that translation-repressed mRNA and miRISC are concentrated in cytoplasmic foci structures termed processing bodies (P-bodies, PBs) for storage or mRNA decay [42]. PBs contain proteins that participate in the regulation of mRNA degradation pathway such as the mRNA decapping enzymes Dcp1/Dcp2, the 5' – 3' exonuclease Xrn1 [43] and the key P-/GW-body subunit, GW182 [44]. PBs are not the ultimate sites of microRNA-mediated degradation; indeed, under different stimuli such as stress signals, stored mRNAs can be released from PBs and they can return to polysome for translation [45] through a mechanism that has not yet been elucidated.

Evidences for translational repression both at the initiation step and at the post-initiation step have been reported [46]. Two different mechanisms of microRNA-mediated repression of translation at the initiation step have been proposed. The first model suggests that microRNAs could interfere with eIF4E recruitment to the 5' – cap structure of the mRNA, thus preventing the activity of this essential translation initiation factor and the subsequent access to mRNA by the translation apparatus [47,48]. In support of this model Kiriakidou and colleagues demonstrated that human Ago2 directly binds the mRNA cap structure by its cap-binding motif similar to that one of eIF4E [49]. In the second model proposed, miRISC could block the assembly of 80S ribosomal complex on mRNA by recruiting eIF6, a factor important in preventing the premature association of 60S ribosomal subunits with 40S subunits [50], thus determining a block in the translation initiation [51]. In addition to these two models, there is a number of studies that concluded that microRNAs could inhibit translation at the post-initiation steps [52,53] by inducing ribosomes to drop off prematurely from mRNAs thus

antagonizing translation elongation. Finally, microRNAs could promote mRNA degradation by inducing deadenylation of the poly-(A)tail, mediated by the interaction between GW182 and the poly(A)-binding protein (PABP) [54,55]. This event is followed by the decapping of the 5' – terminal cap (m^7G) and subsequent mRNA decay (***Fig. 3***).

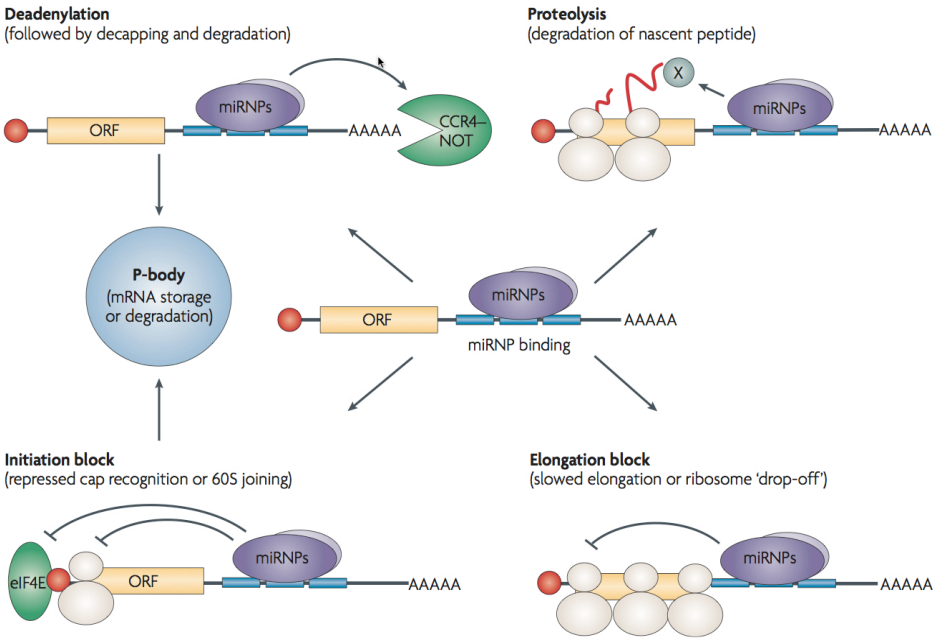

***Fig. 3*: Possible mechanisms of the microRNA-mediated translation repression in animal cells.**

Binding of micro-ribonucleoproteins (miRNPs), possibly complexed with accessory factors, to mRNA 3' UTR can induce deadenylation and decay of target mRNAs (upper left). Alternatively, miRNPs can repress translation initiation at either the cap-recognition stage or the 60S subunit joining stage (bottom left). mRNAs repressed by deadenylation or at the translation-initiation stage are moved to P-bodies for either degradation or storage. The repression can also occur at post-initiation phases of translation, resulting in either slowed elongation or ribosome 'drop-off' (bottom right). Proteolytic cleavage of nascent polypeptides was also proposed as a mechanism of the microRNA-induced repression of protein production (upper-right). A protease (X) that might be involved in the process has not been identified. The 7-methylguanosine cap is represented by a red circle. eIF4E, eukaryotic initiation factor 4E. [Adapted from Filipowicz, 2008, Nature Reviews].

1.1.6 MicroRNA Target Prediction

As previously mentioned, microRNAs can repress translation by binding sequences located in the 3'UTR of mRNAs and several computational algorithms have been developed in order to help the prediction of the targets. These algorithms take into consideration different parameters such as the seed sequence of the microRNA, the number of putative microRNA sites in the target mRNA, the thermodynamics of their interaction, conservation criteria and the context surrounding the mRNA binding sites. Some of the most frequently used computational tools currently available based on conservation criteria are miRanda [56], PicTar [57], TargetScan [58] and DIANA-microT [59]. Other algorithms like PITA [60] or rna22 [61] consider different parameters such as the free energy of the binding between the microRNA seed and the target and the secondary structures of the 3'UTRs.

The computational approach still remains the only source for rapid identification of putative target transcripts, but it is important to note that large discrepancies between results from different algorithms exist. Therefore, it is recommended to use multiple algorithms, and to compare their results in search of shared predictions. Obviously, results from target prediction programs need extensive experimental validation to be eventually confirmed as true microRNA targets.

Related to the overall predictions of microRNAs targets, it is generally thought that the percentage of the comprehensive complementarity between a microRNA and its targets is close to 60%, implying that a single microRNA can regulate many target mRNAs with similar recognition sites. Therefore, a single microRNA can control not only functionally-related targets, but several cellular pathways. Indeed it has been extensively shown that microRNAs can participate in essential processes such as cellular homeostasis, development, differentiation, proliferation, apoptosis and stress responses

[9,62,63]. Additionally, microRNAs can be key regulators in many pathological conditions including autoimmune and neurological disorders, heart and vascular diseases, viral infections and cancer [64].

1.1.7 Multistep regulation of microRNA biogenesis

As mentioned before, more than 60% of human protein-coding genes are regulated by microRNAs: thus, it is not surprising that both microRNA biogenesis and function are subjected to a tight control and the dysregulation of these events is often associated with human diseases.

MicroRNA transcription, processing by Drosha and Dicer, the loading into the RISC complex and microRNA intrinsic regulation such as sequence modification, RNA editing, RNA methylation, microRNA stability are all processes that are strictly regulated as detailed below.

1.1.7.1 MicroRNA transcription regulation

So far only a small number of factors that bind directly to microRNA promoter elements have been identified. Among the RNA Pol II-associated transcription factors p53, V-Myc Avian Myelocytomatosis Viral Oncogene Homolog (MYC), Zinc Finger E-Box Binding Homeobox 1 (ZEB1) and 2 (ZEB2), and myoblast determination protein 1 (MYOD1) have been recently identified and they can positively or negatively regulate microRNA expression [28,65].

1.1.7.2 Drosha and Dicer processing regulation

Several positive and negative processing factors that affect microRNA biogenesis have been identified. Crucial for determining microRNA abundance is the efficiency of Drosha-mediated processing. First of all, post-translational modifications can regulate the protein stability,

nuclear localization and processing activity of the Microprocessor. For instance, phosphorylation of Drosha by GSK3β (glycogen syntetase kinase 3β) is essential for nuclear localization of Drosha [66] and acetylation of Drosha inhibits its degradation [67]; in addition to those, other modifications specifically acting on DGCR8 influence the activity of the Microprocessor. In addition to post-translational modifications, there are several RNA-binding proteins that selectively interact with Drosha and certain pri-microRNAs regulating this step of processing. Among them, the helicases p68 (also known as DDX5, DEAD (Asp-Glu-Ala-Asp) Box Helicase 5) and p72, and receptor-activated SMAD proteins (R-SMADs) SMAD 1 – 3 and SMAD5 [16]. For example, R-SMADs interact with p68 and the stem of pri-microRNAs to stimulate Drosha-mediated processing of miR-21 and miR-199a [68].

Dicer cofactors, such as TRBP, and Ago proteins are subjected to post-translational modifications, which influence Dicer processing and RISC assembly. Moreover, factors that bind directly to specific consensus sequences in the terminal loop of pri- and pre-microRNAs have been discovered. Among them there are the heterogeneous nuclear ribonucleoprotein A1 (HNRNPA1), which facilitates Drosha binding to the pri-microRNA, and the KH-type splicing regulatory protein (KSRP or KHSRP), which promotes both Dicer- and Drosha- mediated processing [16].

1.1.7.3 MicroRNA intrinsic regulation

The events that change RNA sequence or structure can influence microRNAs maturation and turnover. For instance, the presence of single nucleotide polymorphisms (SNPs) can affect microRNA biogenesis and/or its specific targeting [69]; RNA tailing processes (untemplated nucleotididyl addition to the 3' end of RNA) such as uridylation or adenylation modify pre-microRNA and mature microRNA and can facilitate or inhibit microRNA decay [70,71]. The human *let-7* family is the best characterized group of

microRNAs that undergo this type of regulation. In that case LIN28 proteins induce terminal uridylyl tranferases TUT4 and TUT7 to enhance oligouridylation of pre-let-7 blocking Dicer processing and recruiting exonucleases that recognize the U-tail determining microRNA decay [70].

Adenosine to inosine (A-to-I) RNA editing carried out by ADAR enzymes (adenosine deaminases acting on RNA) on specific pri-microRNAs determines the destiny of mature microRNAs in several ways. A-to-I editing in the hairpin region can inhibit the processing of certain microRNAs at the levels of Drosha and Dicer level. Also, RNA editing within the seed region can modify mature microRNA target specificity, leading to the recognition of a new set of target mRNAs [72].

Other modifications such as RNA methylation have been reported: the human RNA methyltranferase BCDIN3D has been shown to *O*-methylate the 5' monophosphate of the pre-miR-145 and pre-miR-23b, essential for Dicer processing thus interfering with this event [73].

Although very little has been known so far about the factor involved in microRNA stability, the regulation of microRNAs turnover could be a major point of control of their abundance in the cell. Several microRNA-degrading enzymes have been identified in different organisms. In *C. elegans*, degradation of unprotected mature microRNAs is performed by the 5'–3' exoribonuclease 1 and 2 (XRN-1 and 2) [74]. In humans, the enzymes XRN1, RRP41 (ribosomal RNA-processing protein 41), and PNPase^{old35} (polynucleotide phosphorylase) have been shown to participate in the turnover of microRNAs [75,76].

Additionally, target mRNAs can modulate the stability of microRNAs: for instance high level of complementarity of the target with a specific microRNA could lead to microRNA degradation accompanied by tailing and trimming [77], but further studies are required to deepen understand the mechanism of target-mediated stability control.

1.1.8 MicroRNAs involvement in human cancer

A significant number of microRNAs can regulate the expression of molecules associated with the cellular fate such as differentiation, proliferation, and apoptosis, implying a critical role for those microRNAs in the fine tuning of these processes and their possible involvement in the multistage events of the carcinogenesis [78]. Therefore more efforts have been done by researches in order to investigate and establish the role of microRNAs in cancer. Indeed microRNAs can affect molecular pathways in cancer development by targeting different oncogenes or tumor suppressors and they can also play a role in cancer-stem-cell biology, angiogenesis, in the epithelial-mesenchimal transition, metastasis and drug resistance [64]. Moreover, in malignant tissues microRNAs can be up or downregulated thus themselves can be considered as oncogenes (oncomicroRNAs) or tumor suppressors, respectively.

Aberrant microRNA expression has been demonstrated essentially in every cancer type in which dysregulated microRNAs often target genes involved in cell proliferation, growth, apoptosis and migration. Hence it follows the importance to identify the alteration of microRNA profile in malignant cells compared to normal cells. Indeed tumors exhibit a specific microRNA signature, named as miRNome, characterizing not only the malignant state of the cells but also their features such as grade, stage, aggressiveness, vascular invasion and proliferation indexes [79].

MicroRNA profiling is a straightforward approach to identify the possible contribution of microRNAs to cancer pathogenesis. It can be performed by using microarrays analyses and reverse transcription followed by PCR (RT-PCR), or next generation sequencing (NGS) and it has been shown that microRNAs expression profile changes in most human cancers [80]. Studies performed using those high through-put technologies resulted in the identification of microRNA signature that allowed classification of cancer

subtypes and of different stages in tumor progression more accurately than standard transcriptome profiling of mRNAs [81]. The great potential of using microRNAs profiling is due to their stability compared to messenger RNAs [82] and to the modern technologies that allow their detection in virtually any type of tissue. Therefore microRNA expression profile can be helpful in diagnostic and prognostic classification of human malignancies and of disease progression.

Altered expression of microRNAs in cancer can result from: chromosomal abnormalities such as genomic amplifications, deletions, mutations or single nucleotide polymorphisms (SNPs) [83,84], epigenetic changes [85], changes in some of the components of the microRNA biogenesis machinery [86] and altered transcription factors activity [87]. Furthermore, the presence of mutations or SNPs in the microRNA binding sites in the 3'UTR of oncogenes are correlated with an increased risk of cancer [88]. As a result of aberrant expression, microRNAs can be involved in the process of tumorigenesis. For example, upregulation of an oncogenic microRNA may lead to inhibition of a tumor-suppressor protein; conversely down-regulation of a tumor-suppressor microRNA can result in an increased expression of an oncogenic protein. The presence of a loss-of-function mutation in a tumor-suppressor microRNA or a mutation in a microRNA binding site in an oncogene mRNA can cause tumorigenesis, due to the lack of regulation of the protein expression. Likewise the presence of a loss-of-function mutation in oncogenic microRNAs or mutation in tumor-suppressor mRNAs can reduce tumorigenesis by an increased expression of tumor-suppressor proteins [64,89] (***Fig. 4***). Understanding the mechanisms underlying these abnormalities could allow the characterization of new biomarkers and the development of new molecular strategies for the therapy of cancer.

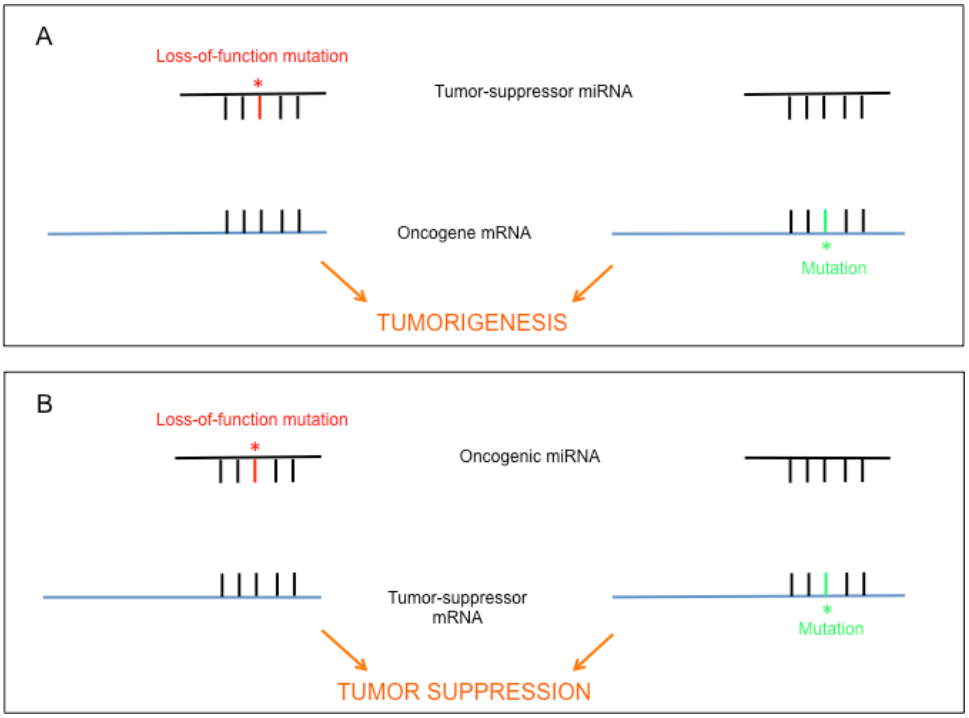

Fig. 4: Example of microRNA dysregulation in cancer.
A *– the presence of a loss-of-function mutation in a tumor-suppressor microRNA or a mutation in an oncogenic mRNA lead to tumorigenesis;* ***B*** *– the presence of a loss-of-function mutation in an oncogenic microRNA or a mutation in a tumor-suppressor mRNA can reduce tumorigenesis by incresing the expression of tumor-suppressor proteins. [Adapted from Kong YW, 2012, Lancet Oncol].*

2. GLIOBLASTOMA

2.1 Glioblastoma: a brief overview

Gliomas are primary malignant tumors developing from cells that support neuronal function in the central nervous system (CNS), in particular the precursors of astrocytes, oligodendrocytes, ependymal cells (collectively named as glial cells) or their progenitors/stem cells [90]. These tumors are named on the basis of their most common elements: astrocytoma, oligodendroglioma, ependymoma or a mixture of lineage termed as oligoastrocytoma.

Astrocytomas account for about 85% of all gliomas and they are classified according to the current World Health Organization (WHO) into four tumor grades (I-IV), from low (grade I) to high (grade IV) on the basis of their histopathologic features such as nuclear atypia, mitotic activity, endothelial hyperplasia and necrosis [91]. Grade IV astrocytoma, also termed as glioblastoma multiforme (GBM) or simply glioblastoma, is the most malignant and the most common brain tumor [92], characterized by rapid proliferation, increased invasiveness and resistance to radio- and chemotherapy [91]. Glioblastoma can develop as a *de novo* neoplasm (primary glioblastoma) or from a lower grade astrocytoma (secondary glioblastoma) and the specific gene mutations that characterized these two subtypes are not definitive [93,94].

The current treatment for glioblastoma includes surgical resection, radiation and Temozolomide (TMZ) chemotherapy. Despite the treatment, the prognosis remains poor, with a median survival of less than 15 months [95,96] with more than half of the patients develop chemoresistance rapidly [97].

One of the major features of glioblastoma cells is their ability to infiltrate the surrounding normal brain, making the margins of the tumor difficult to identify and the surgical removal incomplete. Therefore, understanding the

mechanisms underlying glioma cells invasion is critical to the development of new therapeutic strategies that can improve the existing treatments [91].

2.2 Emerging role of microRNAs as modulators in malignant glioblastoma

Increasing evidences supports a role of microRNAs as key regulators of the events associated with glioblastoma cell biology, thus holding a great potential for these molecules as future therapeutic tools. Indeed, microRNA expression patterns obtained by using genomic profiling techniques are refining glioblastoma classification and differentiation between grades and stages of this tumor [98].

The most common dysregulation of microRNAs observed in glioblastomas seems to be overexpression, based on the systematic literature review published by Moller et al [98]. Among microRNAs found upregulated in glioblastoma, the most extensively investigated are miR-21, miR-10b, miR-221 and miR-222. However, other microRNAs have been found downregulated in glioblastoma, for instance miR-128 [108], miR-29c [113], miR-134 [114].

One of the first microRNA found to be highly expressed in glioblastomas is miR-21, previously characterized as an oncomir in most cancers, as it targets tumor suppressor genes [99]. In Glioblastomas, miR-21 was found not only to be upregulated [100], but its expression correlated with tumor grade and poor prognosis [101]. Another microRNA found to be over-expressed in glioma specimens compared to non-neoplastic brain tissues is miR-10b [102]. This microRNA has a positive effect on proliferation, since its inhibition slowed down glioma cell proliferation through a mechanism that involved cell cycle arrest and apoptosis. Indeed, levels of miR-10b correlated with those of positive cell-cycle regulators as cyclins B1 and D1. Accordingly, it has been postulated that proliferation of glioma could be regulated by miR-

10b through its direct or indirect action on the cell cycle machinery [103]. Interstingly, the cell cycle machinery appears to be a common target for oncomiRs such as miR-221 and miR-222 [104]. Co-suppression of miR-221/222 directly resulted in the up regulation of $p27^{kip1}$, one of the members of cyclin-dependent kinase (CDK) inhibitors, which prevented cell cycle progression from G1 to S phase affecting the growth of glioma cells [105]. Conversely, over-expression of miR-221/222 resulted in a down-regulation of the protein tyrosine phosphatase μ (PTPμ) [106], a member of the type IIb subfamily of receptor PTPs (RPTP), involved in cell invasiveness and adhesion. While a direct effect of those miRNAs on the 3'UTR of PTPμ has not been investigated, down-regulation of this phosphatase has been determined in human glioblastoma [107].

As we previously mentioned, enhanced proliferation by tumor cells can be achieved by upregulating microRNAs or downregulating microRNAs that either have a positive or negative effect on cell cycle, respectively. An example can be provided by miR-128, a microRNA abundant in neurons, which is downregulated in gliomas and is associated with tumor suppressive effects, since its upregulation can significantly reduce glioma cell proliferation *in vitro* and glioma xenografts growth *in vivo* [108]. Among the mechanisms proposed for miR-128 are the ability to reduce glioma stem cell self-renewal by targeting the 3'UTR of the oncogene B lymphoma mouse Moloney leukemia virus insertion region (Bmi-1) [109] and the ability to repress the proliferation of glioma-initiating neural stem cells (giNSCs) by targeting the two oncogenic kinases epithelial growth factor receptor (EGFR) and platelet-derived growth factor receptor alpha (PDGFRα) [110]. In addition, miR-128 can inhibit proliferation of glioma cells by targeting E2F3a, a transcription factor that regulates cell cycle progression [111] and by targeting the tyrosine kinase Wee1, which acts as a negative regulator of entry to mitosis (G2 to M transition) [112].

Other microRNAs downregulated in glioblastomas, such as miR-29c, can arrest the cell-cycle at the G1 stage through repression of the cyclin-dependent protein kinase 6 (CDK6) [113]. Others, like miR-134, can inhibit not only proliferation, but also invasiveness and migration and can increase apoptosis of glioblastoma cells by targeting Nanog transcription factor [114].

As the development of novel therapeutic strategies for glioblastoma treatment is desperately needed, it would be relevant to investigate and to understand the molecular mechanisms by which microRNAs can support or counteract growth and survival of this malignancy.

3. GROWTH DIFFERENTIATION FACTOR 15 (GDF15): A MODULATOR OF TUMORIGENESIS

3.1 GDF15 organization, processing and signaling

Growth differentiation factor 15 (GDF15) is a member of the transforming growth factor β (TGF-β) superfamily, which comprises an expanding group of growth and differentiation factors with a documented role in proliferation, cell-differentiation, inflammation, apoptosis, angiogenesis, adhesion, wound healing and tissue repair [115]. GDF15 is also known as non-steroidal anti-inflammatory drug-activated gene 1 (NAG-1) [116], macrophage inhibitory cytokine I (MIC-I) [117], prostate-derived factor (PDF) [118], placental TGFβ (PTGFβ) [119] and placental bone morphogenetic protein (PLAB) [120,121]. In the brain, GDF15 is reported to be expressed in epithelial cells of the choroid plexus and secreted into the cerebrospinal fluid (CSF) [122].

The human GDF15 gene maps to chromosome 19 in the region p13.1-13.2 and it is composed of two exons separated by a single intron. The gene generates a 308 amino acid precursor protein containing a 29 amino acid signal peptide, a 167 amino acid pro-peptide sequence and a 112 amino acid C-terminal mature domain.

Upon the removal of the N-terminal hydrophobic signal peptide and after disulfide-linked dimerization, the precursor protein is cleaved at the furin-like RRAR proteolytic site [117] resulting in the release of the 112 amino acid mature GDF15 protein, which is then secreted into the extracellular matrix where it is a biologically active disulfide-linked homodimer [123]. The unprocessed precursor protein of GDF15 may additionally be secreted and it can bind to the extracellular matrix (***Fig. 5***) [124].

Similar to other members of the TGF-β family, GDF15 signaling is initiated by the binding to type II TGF-β receptor that leads to the activation

of type I TGF-β receptor through its phosphorylation. Type I receptor then phosphorylates receptor-regulated SMADS that form heterodimers or trimers with common SMAD4 and translocate into the nucleus where they interact with transcriptional factors and regulate the expression of numerous genes [115].

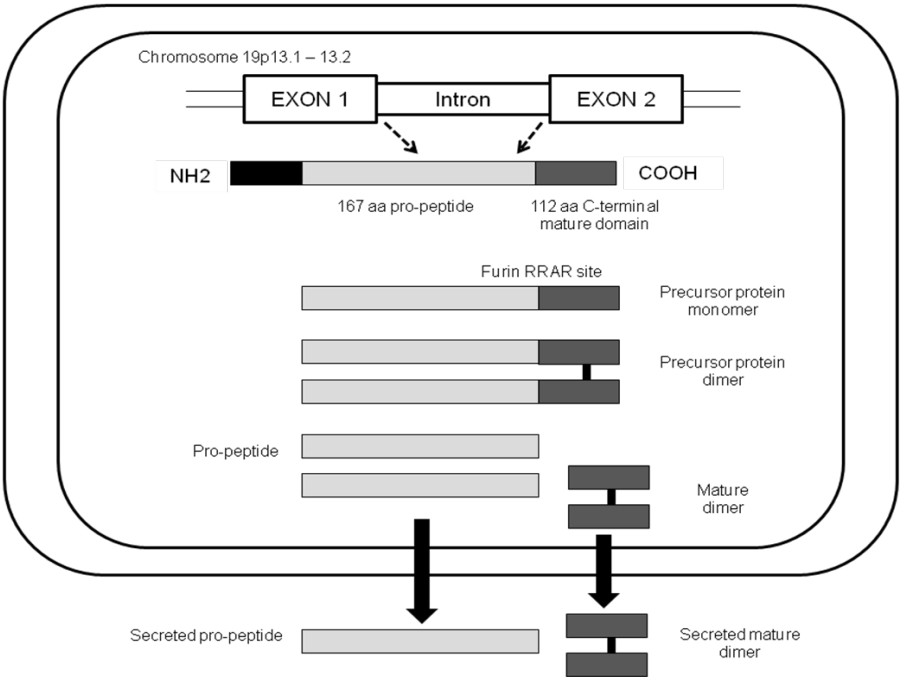

Fig. 5: Processing and formation of mature GDF15 dimer.
GDF15 gene maps to chromosome 19 in the region p13.1-13.2. The gene generates a 308 amino acid precursor protein containing a 29 amino acid signal peptide, a 167 amino acid pro-peptide sequence and a 112 amino acid C-terminal mature domain. Upon the removal of the N-terminal hydrophobic signal peptide and after disulfide-linked dimerization, the precursor protein is cleaved at the furin-like RRAR proteolytic site resulting in the release of the 112 amino acid mature GDF15 protein, which is then secreted into the extracellular matrix where it is a biologically active disulfide-linked homodimer. The unprocessed precursor protein of GDF15 may additionally be secreted and it can bind to the extracellular matrix [Adapted from Mimeault M, 2010, J Cell Physiol].

3.2 GDF15 expression in normal tissues

Although placenta appears to be the only tissue that expresses large amounts of GDF15 under basal physiologic conditions [125], the low basal levels present in many types of resting cells can be dramatically increased in response to different cellular stress signals. These signals include oxygen deprivation (hypoxia and anoxia) [126], short-wavelength light exposure [127], inflammation [119], cardiovascular diseases [128], metabolic disorders [129] and in different types of cancer, including those of the prostate, colon, pancreas and breast [130]. Interestingly, GDF15 can be strongly induced by anti-inflammatory drugs such as Non-steroidal Anti-Inflammatory Drugs (NSAIDs) as well as by several dietary compounds generally resulting in an anti-proliferative phenotype [131].

3.3 GDF15 expression in cancer

During the processes of cancer development and progression GDF15 can play a dual role through both a negative and a positive modulation of cell proliferation, differentiation, migration, invasion, survival and apoptosis [116]. For instance, its expression was downregulated in colon tumors compared to adjacent normal tissue [132], while GDF15 serum levels were found to be elevated in patients with colorectal carcinoma compared to healthy controls [133] and elevated levels of the transcript have been found in the poorly differentiated cells in the sub-mucosa of the invasive areas of gastric cancers [134]. Moreover there are evidences of increasing serum levels of GDF15 in association with disease progression, shorter survival and recurrence [135,136]. In patients with advanced stages of cancer, serum levels of GDF15 can be enhanced from a mean of 0.45 ng/ml to 5 – 50 ng/ml or higher [137]. Noteworthy, GDF15 serum levels higher than 5 – 8 ng/ml cause severe anorexia/cachexia, a cancer-associated weight loss condition, which is common in patients with advanced tumors [129].

The most accepted hypothesis about the dichotomy of GDF15 in cancer cells is that the differential expression of this protein associates with different stages of tumor progression. In particular GDF15 can act as suppressor of tumorigenesis in normal tissue at the early stages of cancer development and it can promote tumor survival and invasiveness at advanced stages of the disease [138].

3.4 Regulation of GDF15 expression

The human GDF15 promoter contains several *cis-acting* and *trans-acting* elements that can be regulated by numerous transcription factors and mechanisms and modulated by anti-tumorigenic compounds. Previous studies have indeed demonstrated that the increased GDF15 expression after anti-cancer treatments could be mediated by the transcription factors Sp-1, p53, early growth response protein 1 (Egr-1) [116,139], NF-kB [140], poly (ADP-ribose) polymerase-1 [141] and hypoxia-inducible factor-1α (HIF-1α) [142]. In addition, it has been observed an increase of both GDF15 protein and mRNA by inhibiting the PI3K/AKT/GSK-3β pathway, which is involved in the regulation of cell-survival, proliferation and growth, thus suggesting that GDF15 can alter these processes [143]. Feng and colleagues have additionally demonstrated that Calumenin-15 (Calu-15) facilitates filopodia formation and consequently migration of cells by increasing transcription of GDF15 through the binding to its promoter region [144].

3.5 GDF15 in glioblastoma

Increased GDF15 mRNA expression has been reported in gliomas of patients during malignant progression to glioblastoma [145], thus implying the identification of GDF15 as an interesting candidate biomarker. In support

of this hypothesis, elevated levels of GDF15 have been found in the CSF of patients with glioblastoma [146].

In addition to compounds mentioned above, numerous chemicals with anticancer properties are able to up-regulate GDF15 expression suggesting multiple mechanisms responsible for its induction [147,148,149]. Specifically related to glioblastomas, there are numerous experimental results showing an up-regulation of GDF15 expression in glioblastoma cells in response to cytotoxic stimuli, such as chemotherapy treatments and anti-tumorigenic compounds with a wide range of chemical structures [148,150].

Our laboratory has previously reported an increased expression level of GDF15 in the LN-229 glioblastoma cell line following the treatment with fenofibrate, an agonist of peroxisome proliferator activated receptor alpha (PPARα) [148].

4. FENOFIBRATE

4.1 Molecular action of fenofibrate

Fenofibrate belongs to the fibrates' class of lipid-lowering drugs. It has been used for more than 20 years to treat endogenous hyperlipidemias, hypercholesterolemias and hypertriglyceridemias, both as monotherapy and as component of combination therapy [151]. Interestingly, fenofibrate has been extensively used to reduce the levels of triglycerides and cholesterol in plasma, to improve LDL: HDL (Low Density Lipoprotein: High Density Lipoprotein) ratio, and to counteract the process of atherosclerosis through the regulation of apolipoprotein expression [152]. Fenofibrate is rapidly hydrolyzed *in vivo* to fenofibric acid, its active metabolite, which is also responsible for the effects of the drug mentioned above. Fenofibrate is a protein-bound, lipophilic compound (2-(4((4-chlorobenzoyl) phenoxy)-2-methyl-propanoic acid, 1-methylethyl ester)) activated via the hydrolysis of

the compound's ester bond [153]. Generally, fibrates are considered being well tolerated with a low incidence of toxicity in almost every organ.

The effects of fenofibrate to modulate genes involved in lipid metabolism are a consequence of its ability to activate peroxisome proliferator-activated receptors (PPARs). In particular, fenofibrate is a potent synthetic ligand for PPARα, which has been initially discovered as a regulator of glucose and lipid metabolism. Moreover PPARα activation results in anticancer properties [154].

The activation of PPARα by fenofibrate determines an increasing activity of malonyl-CoA decarboxylase enzyme, that in turn inhibits malonyl-CoA and thus decreases the inhibition of carnitine palmitoyl transferase I (CPT-1), responsible for transferring free fatty acyl (FFA) groups into the mitochondria. This event stimulates fatty acids β-Oxidation and induces a shift of metabolism towards the glycogenesis by increasing the concentration of Acetyl-CoA, which inhibits the pyruvate dehydrogenase (PDH) activity (***Fig. 6***) [153].

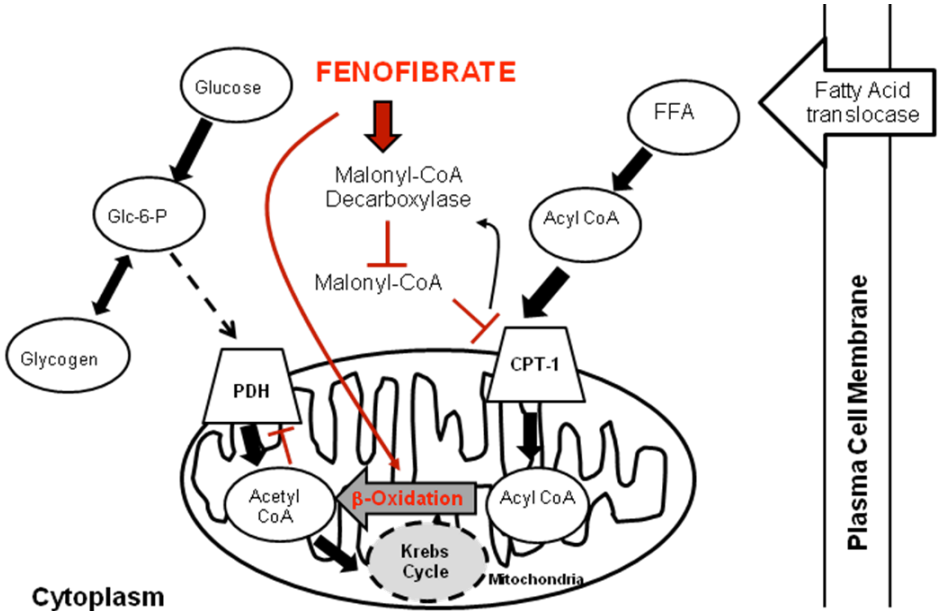

Fig. 6: Role of fenofibrate in regulating fatty acids metabolism
PPARα activation by fenofibrate determines an increasing activity of malonyl-CoA decarboxylase enzyme, that in turn inhibits malonyl-CoA and thus decreases the inhibition of carnitine palmitoyl transferase I (CPT-1), responsible for transferring free fatty acyl (FFA) groups into the mitochondria. This event stimulates fatty acids β-Oxidation and induces a shift of metabolism towards the glycogenesis by increasing the concentration of Acetyl-CoA, which inhibits the pyruvate dehydrogenase (PDH) activity.

4.2 Role of PPARα agonist fenofibrate in anticancer treatment

PPARα, the first PPAR to be identified [155], is a nuclear receptor that belongs to the steroid hormone receptor superfamily. Similarly to the other two isoforms PPARβ/δ and PPARγ, PPARα acts as a ligand-activated transcription factor. The PPARs signaling start with the binding of agonist ligands to PPAR receptor, which in turn triggers heterodimerization of this receptor with the 9-*cis*-retinoic acid receptor (RXR) and recruits the transcriptional machinery to activate PPARα-responsive genes, a process

known as “transactivation” [156]. The heterodimer PPAR/RXR binds specific responsive elements (REs) in the regulatory regions of target genes, termed peroxisome proliferator response elements (PPREs) which are composed of two direct hexanucleotide repeats spaced by one nucleotide (AGGTCA-n-AGGTCA) [156]. The endogenous ligands that activate PPAR family receptors derive from fatty acids metabolism and other dietary compounds, hence emphasizing their important role in regulating the expression of genes involved in glucose and lipid metabolism [157].

PPARα is expressed in many tissues, in particular those that require fatty acid oxidation as a source of energy. While the primary role of PPARα is to increase the cellular capacity to catabolize fatty acids [158], several studies suggest that activating PPARα could be useful for the prevention and treatment of different cancers. Indeed, PPARα ligands have both direct anti-tumor and anti-endothelial effect *in vitro* [159]. In particular fenofibrate has been shown to possess a strong suppressive activity on the proliferation of melanoma, breast carcinoma and Lewis lung carcinoma cell lines [154,160]. Moreover fenofibrate has been shown to be able to inhibit the secretion of tumor-secreted growth factors such as Vascular Endothelial Growth Factor (VEGF) in glioblastoma [159].

Two potential anti-tumorigenic PPARα-dependent pathways have been proposed [158]. First, by inhibiting NF-kB-dependent signals such as the production of pro-inflammatory cytokines [161], key factors known to contribute to inflammation-driven carcinogenesis [162]; second, by negatively regulating the *Warburg effect* exhibited by the tumor cells, thus interfering with their metabolic pathway. The *Warburg effect* is the process by which despite the presence of aerobic conditions, tumour tissues metabolize approximately ten-fold more glucose to lactate in a given time than normal tissues [163]. Therefore, the activation of PPARα by its endogenous or exogenous ligands has two main effects: it can increase

mitochondrial oxidation of fatty acids thus depleting the lipid stores [164], and it can inhibit the expression of glutaminase, which decreases glutamine levels [165]. Thus, according to Otto Warburg's discovery about the distinctive dependency of tumor cell metabolism from glycolysis, PPARα activity induced by fenofibrate should affect glycolysis/glutaminolysis by causing a severe energy deficit, which then results in reduced proliferation and induction of cell death [166].

4.3 Fenofibrate-induced apoptosis in glioblastoma

In cell culture studies as well as in animal studies, members of fibrate family were shown to possess anticancer properties. Treatment of glioblastoma cells with ligands of PPARα (bezafibrate, gemfibrozil) determines growth arrest and activates apoptotic response [167]; fenofibrate has been shown to induce apoptosis and decrease proliferation rate in endometrial cancer cells [168] and in human and mouse medulloblastoma cells lines [152]. Despite these observations, molecular mechanism(s) of fenofibrate activity on cancer cells are not fully understood and it has not yet been elucidated what role PPARα has in the antiproliferative effect of this drug. Nevertheless, several studies have shown PPARα-independent activities of fenofibrate: for example by inhibiting Akt signalling pathway [154], by attenuating IGF-I mediated growth responses [152], by inhibiting endothelial cell growth and angiogenesis [159,169]. In addition to these observations, PPARα-independent effects on mitochondrial respiration [170] and on cell motility or gap-junction intercellular coupling have been reported [171].

There is evidence of dose-dependent and time-dependent actions of fenofibrate in LN-229 human glioblastoma cell-line, which is positive for PPARα expression. Wilk and colleagues have indeed demonstrated that

treating LN-229 cells with 25μM of fenofibrate resulted in G_1 cell cycle arrest together with marginal levels of dead cells at 72 hours. Conversely, treatment with 50μM of fenofibrate resulted in extensive cell-death percentage within 72 hours. The observed delayed apoptotic effect of fenofibrate has been shown to be preceded by the nuclear retention and serine phosphorylation of the transcription factor FOXO3A, a member of the *forkhead-box O* transcription factors, resulting in the Fox-O dependent up-regulation of the pro-apoptotic gene *Bim* (BCL2 Like 11). Moreover, LN-229 treatment with siRNA against PPARα only partially rescued the cells from fenofibrate effects, suggesting that both PPARα-dependent and PPARα-independent mechanisms might be responsible for the activation of the pro-apoptotic axis FOXO3A/BIM [172].

5. THE GDF15 CO-ENCODED miR-3189

We have previously found that treatment of LN-229 glioblastoma cells with fenofibrate result in increased expression of GDF15 [148].

In this study, we have analyzed the genomic sequence of GDF15 and found that contains a microRNA, miR-3189, encoded within its single intron at a position proximal to exon 1. The precursor sequence encoded by miR-3189 contains two mature microRNA sequences within the stem-loop: miR-3189-3p and -5p, of 21 and 25 nucleotides in length, respectively (***Fig. 7***). The biological function of this microRNA has never been described before.
Because of the role of microRNAs in gene regulation, we sought to define the effects of these co-expressed microRNAs, miR-3189-3p and miR-3189-5p, in the biological function of GDF15. The following results have been enclosed in a manuscript submitted for publication (Duane Jeansonne*, Mariacristina De Luca*, Luis Marrero, Adam Lassak, Marco Pacifici, Dorota Wyczechowska, Anna Wilk, Krzysztof Reiss and Francesca Peruzzi. Anti-

Tumoral Effects of miR-3189-3p in Glioblastoma. * Authors contributed equally).

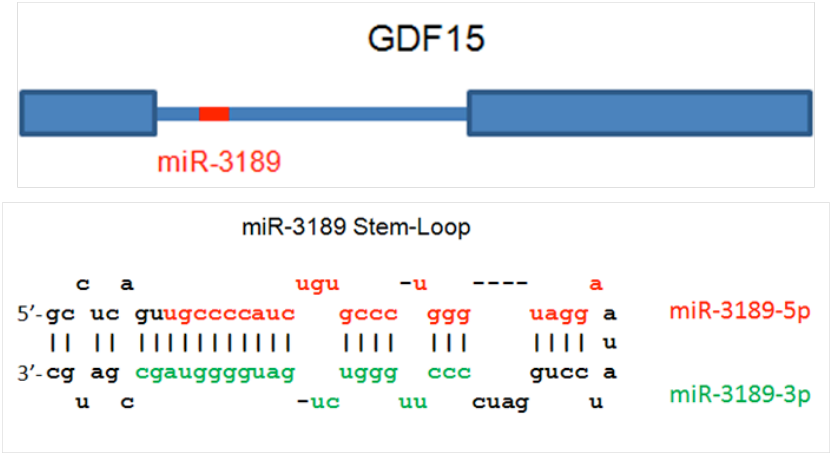

Fig. 7: *Schematic of the GDF15 gene: the gene encoding GDF15 is composed of a single intron, which contains microRNA-3189 at a position proximal to exon 1*

5.1 SF3B2 splicing factor and p63RhoGEF are targets of miR-3189-3p

According to TargetScan Prediction database (www.targetscan.org) the major predicted gene targets for miR-3189-3p are the splicing factor SF3B2 (splicing factor 3b, subunit 2, 145 kDa) and the guanine nucleotide exchange factor p63RhoGEF (Rho guanine nucleotide exchange factor (GEF) 25). These two transcripts have respectively two seeds (one conserved and one poorly conserved) and three seeds (one conserved and two poorly conserved) for miR-3189-3p in their 3' UTR.

5.1.1 The RNA spliceosomal subunit SF3B2

In mammals there are two different spliceosome complexes: the major (U2-type) and the minor (U12-type). They recognize different classes

of splice sites and they have a different small nuclear ribonucleoproteins (snRNP) composition [173].

SF3B2 is one of the four splicing-associated proteins (SAPs) of the 450 kDa SF3b complex [174], a key factor that takes part in both splicing pathways and it participates to the assembly of the pre-splicing complex [173]. SF3B2 is also named SAP145 (U2 snRNP-associated spliceosomal protein 145), and it has been suggested to interact with SAP49 in a U2 snRNP-associated complex that works to tether U2 snRNP to the branchpoint sequence (BPS) in the introns [175].

Although very little has been known so far about the role of SF3B2 (and in general about the spliceosomal subunits) in relation to cancer disease, it is gaining attention due to its participation in cell-cycle progression. Indeed there are some different studies demonstrating the existence of a regulatory link between the splicing factors and the events of the cell-cycle. Of interest, by studying the interaction between the Human Immunodeficiency Virus Type 1 VPR protein and host cell proteins, Terada and colleagues have found that Vpr colocalizes with SF3B2 in the splecked distribution and interferes with SF3B2 function leading to checkpoint-mediated G2 cell cycle arrest [176]. Furthermore, it has been reported that by inhibiting the induction of SF3B2 there is a marked reduction in the percentage of T cells that entered S-phase, but they are still able to increase in size [177].

5.1.2 The guanine nucleotide exchange factor p63RhoGEF

The 580 amino acids p63RhoGEF protein (63 kDa) has been demonstrated to belong to the DBL family of guanine nucleotide exchange factors (GEF) based on sequence homology criteria with the *Dbl* oncogene [178]. Rho-GEFs have the function to catalyze the conversion of the small RHO GTPases (as RHOA, RAC1 and CDC42) from the inactive GDP-bound

form to the active GTP-bound form. As the other GEFs, it is characterized by the presence of a DBL homology (DH) domain in tandem with a pleckstrin homology (PH) domain [179]. It is expressed mainly in the heart and the brain (particularly astrocytes and oligodendrocytes) and to activate the formation of stress fibers in fibroblasts and cardiomyocyte-derived H9C2 cells specifically acting as a GEF for RHOA protein [178]. p63RhoGEF is an effector of the $G\alpha_q$ subfamily of heterotrimeric guanine nucleotide–binding proteins (G proteins) and thus it links G protein–coupled receptors (GPCRs) to the activation of RHOA and to the control of the actin cytoskeleton reorganization [180]. It has been clearly demonstrated that p63RhoGEF specifically displayed GDP/GTP exchange activity towards RHOA, but not towards the other two Rho GTPases RAC1 and CDC42 [178]. The full-length p63RhoGEF form of the protein and the N-terminally truncated form, known as GEFT, are encoded from the same gene and they co-exist within a single cell type. The splice variant GEFT misses the first 105 amino acids. However, both isoforms have the ability to activate RHOA, but not RAC1 and CDC42 and induce the formation of actin stress fibres in several cell types [181]. The two variants differ for their localization, due to the lack of the N-terminal 105 amino acids in GEFT. Specifically, while p63RhoGEF localizes in the plasma membrane, GEFT is preferentially found in the cytoplasm [182]. The subcellular localization appears to determine the function of p63RhoGEF, which has a crucial role in serum-induced migration through the formation of a single polarized lamellipodial protrusion in response to serum stimulation. Consequently, knockdown of p63RhoGEF can suppress the chemotactic migration of MDA-MB-231 human breast carcinoma cells toward serum, but had no significant effect on the chemokinetic response [183].

AIM OF THE STUDY

Glioblastoma is one of the most aggressive brain tumors. Here, we found that expression levels of Growth Differentiation Factor 15, GDF15, and its co-encoded miRNA, miR-3189-3p, were increased by treatment of glioblastoma cells with fenofibrate, a lipid-lowering drug with multiple anticancer activities. In the same experimental setting, functionality of miR-3189-3p was tested by RNA binding protein immunoprecipitation, and miR-3189-3p co-immunoprecipitated with Argonaute 2 together with two of its major predicted gene targets, the SF3B2 splicing factor and the guanine nucleotide exchange factor p63RhoGEF. Overexpression of miR-3189-3p resulted in a significant inhibition of cell proliferation and migration through direct targeting of SF3B2 and p63RhoGEF, respectively. In astrocytomas and glioblastomas clinical samples the expression of GDF15 was upregulated, while levels of miR-3189-3p where decreased compared to controls. This attenuated expression of miR-3189-3p paralleled elevated expression of SF3B2, which could contribute to the activation of SF3B2 growth promoting pathway in these tumors. Finally, miR-3189-3p-mediated inhibition of tumor growth *in vivo* further supported the function of this microRNA as a tumor suppressor.

MATERIALS AND METHODS

Cell culture, transfection, and reagents

LN-229 cells were obtained from the American Type Culture Collection (CRL-2611; Manassas, VA) and cultured under standard growth conditions. Fenofibrate was from Sigma (St. Louis, MO). MiR-3189-3p mirVana microRNA mimic and miR-3189-3p mirVana microRNA Inhibitor (anti-miR-3189-3p) were purchased from Life Technologies. For transfection experiments, cells were seeded at a density of $4x10^5$ cells/60 mm dish or $2.5x10^4$ cells/well in a 12-well plate, and transfected using Lipofectamine 2000 (Life Technologies, Grand Island, NY) following manufacturer's instructions. For Ago2-IP experiments, cells were plated in complete medium (DMEM+ 10%FBS) at the concentration of 1.1x106/100 mm dish and treated with 50 μM of Fenofibrate for 48h. SF3B2 siRNA, p63RhoGEF siRNA, and Control siRNA were were purchased from Santa Cruz (Dallas, TX). PPARα siRNA was purchased from Thermo Scientific (Waltham, MA). PPARα inhibitor (GW 9962) was purchased from Enzo Life Science (Farmingdale, NY).

Quantification of microRNAs and mRNAs Expression Levels

Total RNA was isolated using mirVana^{TM} microRNA Isolation Kit (Ambion Life Technologies Co., Grand Island, NY) and subsequently 500 ng of total RNA were reverse transcribed using TaqMan® MicroRNA Reverse Transcription kit (Applied Biosystems Life Technologies Co., Grand Island, NY). The reactions were incubated for 30 min at 16 °C, 30 min at 42 °C, and 5 min at 85 °C. microRNAs expression levels were determined using TaqMan® 2X Universal PCR Master Mix (Applied Biosystems Life Technologies Co., Grand Island, NY), following the manufacturer's protocol. Each generated cDNA was amplified using the Light Cycler 480 qPCR system (Roche, Basel, Switzerland). The reactions were incubated for 10

min at 95°C, 50 cycles of 15 sec at 95°C and 1 min at 60°C. RNU6B was used as reference gene.

For mRNA quantification, 500 ng of total RNA were reverse transcribed using High Capacity cDNA Reverse Transcription Kit (Applied Biosystems Life Technologies Co., Grand Island, NY). The reactions were incubated for 10 min at 25 °C, 120 min at 37 °C, and 5 min at 85 °C. 50 ng of cDNA were used to quantify by TaqMan® 2X Universal PCR Master Mix (Applied Biosystems Life Technologies Co., Grand Island, NY) the expression level of GDF15, SF3B2, p63RhoGEF and PPARα. GAPDH was utilized as reference gene. The reactions were incubated for 10 min at 95°C, 50 cycles of 15 sec at 95°C and 1 min at 60°C. The relative quantification of gene expression was calculated using the comparative Ct ($2^{-\Delta\Delta Ct}$) method.

RNA extraction from formalin-fixed paraffin-embedded (FFPE) tissues

The RNA extraction from FFPE tissues of normal control, astrocytoma and glioblastoma clinical samples, was performed by using the RNeasy FFPE kit from Qiagen (Valencia, CA) following the manufacturer's procedure. For mRNA and microRNA expression quantification it was followed the same protocol described above. For the clinical samples relative quantification was represented as $1/\Delta Ct$ to maintain real differences in Ct values between samples.

Western Blots

LN-229 cells were collected by gently scraping in the presence of cold PBS, following by centrifugation and disruption of the cell pellet in lysis buffer (50 mM Hepes pH 7.5, 150 mM NaCl, 1.5 mM $MgCl_2$, 1 mM EGTA pH 8.4, 10% glycerol, 1% Triton-X-100) containing 1 mM of Protese Inhibitor Cocktail (Sigma-Aldrich, St. Louis, MO), 1 mM of PMSF (Sigma-Aldrich, St.

Louis, MO), 1 mM of phosphatase Inhibitor (Sigma-Aldrich, St. Louis, MO) and 1 mM of sodium orthovanadate. Whole-cell lysates (50 to 100 µg) were electrophoresed on a 4-15% SDS-PAGE gel (Mini-PROTEAN TGX^{TM} Precast Gel, Biorad, Hercules, CA) and transferred to a 0.2 µm nitrocellulose membrane (BioRad, Hercules, CA) using the Trans-Blot TURBO^{TM} apparatus (BioRad, Hercules, CA). Mouse anti-SF3B2 and rabbit anti-14-3-3 were purchased from Santa-Cruz (Dallas, TX), mouse anti-Ago2 was purchased from Millipore (Billerica, MA), rabbit anti-P63RhoGEF antibody was obtained from GeneTex (Irvine, CA), rabbit anti-GDF15 and rabbit anti-E2F-1 antibodies were purchased from Cell Signaling Technology (Beverly, MA), mouse anti-GRB2 was obtained from BD Transduction Laboratories (San Jose, CA).

ELISA assay

Mature GDF15 was detected in the cell culture medium using the GDF15 Quantikine ELISA kit from R&D Systems (Minneapolis, MN), according to the manufacturer's instructions. Sample absorbance was measured at 450 nm using a Bio-Rad Benchmark Plus microplate reader.

RNA-binding protein Immunoprecipitation (RIP)

RIP assay was performed using Ago2 antibody form Millipore (RIPAb+Ago2 RIP). This kit includes negative control mpuse IgG antibody and control primers specific for human FOS, which were utilized for the optimization of Ago2-IP in our cellular model.

$5x10^6$ of LN-229 cells were used for Ago2-Immunoprecipitation and $5x10^6$ cells for the IgG isotype control; $1x10^6$ cells were used for the extraction of total RNA and $1x10^6$ cells for total protein lysates. Cells were washed twice with cold DPBS (Gibco Life Technologies Co., Grand Island, NY), collected by gently scraping with 2 ml of DPBS and centrifuged for 5 minutes, 300xg,

at 4°C. The cell pellet was resuspended in 500 µl of Lysis Buffer (150 mM KCl, 25 mM Tris-HCl pH 7.4, 5 mM EDTA, 0.5% NP40, 5 mM DTT) supplemented with 1 mM of Protease Inhibitor Cocktail, 1 mM of PMSF, 1 mM of Phosphatase Inhibitor, 1 mM of sodium orthovanadate and 100 U/ml of RNAse Inhibitor (Applied Biosystems Life Technologies Co., Grand Island, NY). After 30 minutes of incubation on ice, lysates were spun at 4°C for 30 minutes at 14.000 rpm in a microcentrifuge.

30 µL of Pierce Protein A/G Magnetic Beads (Thermo Scientific, Waltham, MA) were washed three times with 1 ml of Blocking Solution (0.5% BSA dissolved in PBS+/+). The beads were resuspended in 250 µL of Blocking Solution and incubated for 1 h at 4°C with 5 µg of anti-Ago2 mouse monoclonal IgG1k Antibody or with isotype IgG1k control Antibody. The immunocomplexes were washed three times with 1 ml of Blocking Solution and incubation with specific lysates was carried out overnight at 4°C. Next day, the immunocomplexes were washed three times with 500 µL of Lysis Buffer supplemented with the inhibitors. Left-over IP samples before the first wash were collected to determine the efficiency of depletion of Ago2 from the cellular lysate. After the last wash, immunocomplexes were resuspended in 40 µL of Lysis Buffer, of which 20 µL were used for the RNA extraction and 20 µL for Western blot analysis.

RNA extraction from the beads and from the left-over samples was performed using the mirVana^{TM} microRNA Isolation Kit (Ambion Life Technologies Co., Grand Island, NY) followed by reverse trancription and Real-time PCR for mRNAs and microRNAs as described above.

The calculations of fold enrichments of the Ago2-IP samples were done according to a recent published work by Curtale et al [184].

Cloning of the p63RhoGEF and SF3B2 open reading frames

Total RNA was isolated from LN-229 cells and reverse transcribed to cDNA using the High Capacity cDNA Reverse Transcription kit. The cDNA sequence corresponding to the open reading frame (ORF) of p63RhoGEF was PCR amplified. The primers used were: forward, 5' - GGTGGAATTCTGCAGATATGCGGGGGGGGCACAAA and reverse, 5' - CCACTGTGCTGGATTTACAGCTCATCTTCATCCAGCTTGG. Sequences compatible with pcDNA3.1(+) are underlined. Next, the pcDNA3.1(+) vector was digested with EcoRV. This vector and the PCR product (above) were digested with the Klenow fragment of DNA polymerase I to generate single-stranded 3'-overhangs compatible between the two DNA molecules. These products were annealed by incubating at incremental reducing temperatures from 95ºC to 45ºC using a PCR cycler (Bio-Rad). The ORF sequence corresponding to the SF3B2 gene was also cloned into the pcDNA3.1(+) vector using the approach described above. The primers used were: forward, 5' - GGTGGAATTCTGCAGATATGGCGACGGAGCATCCC and reverse, 5' CCACTGTGCTGGATCTAAAACTTGAACTCCTTATATTTCTTGCTGCC. Sequences compatible with pcDNA3.1(+) are underlined.

Cloning for microRNA Functional Analysis

The genomic sequence corresponding to the 3' UTR of p63RhoGEF was PCR amplified from LN-229 cells. This PCR product was ligated into the multiple cloning sites downstream of the Renilla luciferase reporter gene in the psiCHECK-2 vector (Promega, Madison, WI). This vector also contains a firefly luciferase reporter sequence, which allows for normalization of transfection efficiency. The primers used were: forward, 5' - CCGCTCGAGCTGGTGAAAACCATGGGGGTG, containing the XhoI restriction site and reverse, 5' -

ATAAGAATGCGGCCGCGCAGCCTCGGTGATATAACAAAACC, containing the NotI restriction site. The genomic sequence corresponding to the 3’ UTR of SF3B2 was also cloned into the psiCHECK-2 vector. The primers used were: forward, 5’-CCGCTCGAGTTCAAGTTTTAGGTCCCCTCAC, containing the XhoI restriction site and reverse, 5’-ATAAGAATGCGGCCGCGGAGGCTCAGGAGTGTTAAATATTCATCTC, containing the NotI restriction site. The XhoI and NotI restriction sites are underlined.

Mutations of the miR-3189-3p putative binding sites in the p63RhoGEF and SF3B2 3’UTR sequences were generated using the QuikChange Lightning site-directed mutagenesis kit (Agilent Technologies, Santa Clara, CA) using the respective psiCHECK2/3’UTR plasmids as a template.

The oligonucleotides for the mutagenesis of p63RhoGEF sites were as follows: site 1 forward, 5’ – TCAGCCGCCTATTCCCCTTCCAGCTTCAGGGCAGTCCT, site 2 forward, 5’ – TGGAGGAGAACACCTAGACCCTTCCACTTTTTTCTGCCCA AGGAAC, and site 3 forward, 5’ – CCCAAGGACTTTTTTCTGCCCTTCCAACACAGTTTCCTTCAGCTCC.

The oligonucleotides for the mutagenesis of SF3B2 sites were: site 1 forward, 5’ – GAACCACCTCTCCCGCAGTTCCCTTCCACTTGTCATTTCATGTTCTTAT, and site 2 forward, 5’ – GACCTGTTTTGTAAATAAAGCTGTTTCCCTTCCAAAGAGATGAATATTTA ACACTCCTGAGC.

Mutated bases in the miR-3189-3p binding sites were underlined. The reverse oligonucleotide primers were complementary to the forward primers.

Dual Luciferase Assay

LN-229 cells were plated at a density of 8 x10^4 cells/well in a 12-well plate and transfected with psiCHECK-2 vector expressing target 3'UTR (160 ng/well) alone, target 3'UTR with miR-3189-3p mimic (30 nM), or target 3'UTR with microRNA mimic and anti-miR-3189-3p (50 nM) using Lipofectamine 2000. After 24 h, cells were harvested and lysates were assayed for luciferase activity with the Dual-Luciferase Reporter Assay System (Promega) using a Synergy 2 microplate reader (BioTek Instruments, Inc., Winooski, VT). Relative units of Renilla luciferase activity were normalized to the firefly luciferase internal control in each sample. Experiments were performed in duplicate.

Generation of stable LN-229 expressing SF3B2, p63RhoGEF or miR-3189-3p

In order to produce stable LN-229 expressing respectively SF3B2 and p63RhoGEF, LN-229 cells were plated at a density of 1x10^6 cells/100mm dish and transfected with pcDNA3.1(+) containing the ORF of SF3B2 or p63RhoGEF using the empty vector as control. After 24h the selecting antibiotic G418 (Gemini Bio-products, Sacramento, CA) was added at the concentration of 1 mg/ml and the medium was replaced every two/three days complete of fresh antibiotic. The cells were splitted far in order to permit the formation of isolated colonies. When the drug-resistant colonies were large enough, they were transferred into a 12-well plate by using the cloning cylinders and cultured with G418 at the maintenance concentration (0.8 mg/ml). The cells were transferred in plates progressively bigger and the screening of the best clone expressing the biggest amount of the gene of interest (GOI) was conducted by western blot analysis.

For the generation of stable LN-229 expressing the miR-3189-3p, the "Tet-On® 3G Inducible Expression Systems" from Clontech (Mountain View,

CA) was followed. The sequence of the mature miR-3189-3p was cloned in the inducible pTRE3G-IRES vector. A previously generated LN-229 clone with stable expression of the regulator plasmid pCMV-TET3G producing the Tet-On 3G protein was transfected at the density of $1.8x10^5$ in a 6-well plate with the pTRE3G-IRES-miR-3189-3p vector and the linear Hygromycin B marker. The cells were cultured in presence of both G418 and Hygromycin B following the manufacturer's protocol and the clones were grown as described above. The screening of the best clone was performed by Realtime PCR analysis of the expression level of miR-3189-3p in presence and in absence of Doxocyclin in the cultured cells.

Cell Proliferation Assay

LN-229 cells were plated at a density of $2.5x10^4$ cells/well in a 12-well plate and transfected with mock or miR-3189-3p mimic +/- anti-miR-3189-3p. At 72 h after transfection, cells were incubated with medium containing 3-(4,5-dimethylthiazol-2-yl)-5-(3-carboxymethoxyphenyl)-2-(4-sulfophenyl)-2H-tetrazolium (MTS) reagent (Promega) diluted according to manufacturer's instructions. Cells were then incubated at 37°C for 30-60 min and absorbance was measured at a wavelength of 490 nm using a Bio-Rad Benchmark Plus microplate reader.

Cell Cycle Analysis

Cells were collected 48h after transfection and fixed in 70% ethanol overnight at -20ºC. Cells were then centrifuged at 300xg, resuspended in 150 µL of Guava Cell Cycle reagent (Guava Technologies, Hayward, CA), and stained for 45 min at 25ºC while protected from light. Cells were counted by flow cytometry using a FACSAria (BD Biosciences). Cell cycle distribution was evaluated using the ModFit LT program (Verity Software House, Topsham, ME).

Scratch Assay

LN-229 cells were transfected with miR-3189-3p and plated in a 35 mm glass bottom dish (MatTek Corporation, Ashland, MA) at a density of $1.8x10^5$ cells/dish. The scratch assay was performed by moving a pipette tip across the cell monolayer. Migration into the cell-free area was monitored for up to 24h using live cell time-lapse imaging in a VivaView FL incubator fluorescent microscope (Olympus, Center Valley, PA).

In vivo tumor growth

Mice used for in vivo tumor growth studies were female Fox1nu athymic nude mice at 6-7 weeks of age (Harlan Laboratories, Inc., Indianapolis, IN). For the subcutaneous tumor growth, 5 mice per group were injected on the flank with $2x10^6$ LN-229 glioblastoma cells stably expressing the mCherry fluorescent protein and mock-transfected, or transfected with miR-3189-3p mimic. The experiment was repeated using U87MG glioblastoma cells.

For the intracranial injection of U87MG cells, 5 mice per group were injected with 25000 cells stably expressing the Luciferase and mock-transfected, or transfected with miR-3189-3p mimic. All experiments were performed in accordance with institutional ethical guidelines.

In vivo imaging tumors

In vivo growth of LN-229-mCherry and U87MG-luciferase tumors was quantified by biophotonic imaging using a Xenogen IVIS 200 system (Xenogen, Palo Alto, CA). Prior to imaging, mice were placed in the chamber of an XGI-8 vaporizer and anesthesia was induced with 4% isoflurane gas. Anesthesia was sustained inside the imaging chamber using nose cones. Images were captured and quantified with Living Image 4.1 software based

on equivalent regions of interest over the lower back of the mouse. Image intensities were expressed as photon flux per second, square centimeter and surface radiance (photons/sec/cm^2/sr).

Statistical analysis

Data are presented as mean ± SD. Comparison between two experimental groups was performed using the Student's t-test. P-values ≤ 0.05 were considered statistically significant.

RESULTS

Expression of GDF15 is increased after fenofibrate treatment

Previous reports have demonstrated that GDF15 expression is induced following treatment by a variety of chemotherapeutic agents [150,169]. In line with these findings, it has also reported in our laboratory that this gene is upregulated in a microarray analysis of glioblastoma cells treated with the metabolically active anticancer compound, fenofibrate [172]. Fenofibrate is a potent agonist of peroxisome proliferator activated receptor alpha (PPARα), which has exceptional anticancer properties, especially in tumors of neuroectodermal origin, including glioblastomas [148]. To further analyze the effects of fenofibrate on this gene, we have exposed the human glioblastoma cell line, LN-229, to 50 μM fenofibrate and monitored the expression of GDF15 at 24 and 48 hour time points. Following the treatment, total RNA was extracted and subjected to quantitative real-time PCR (qRT-PCR) using GDF15-specific and GAPDH-specific primers. The results in ***Fig. 8A***, show a 60-fold upregulation of GDF15 gene expression. In agreement with these findings, a large increase in GDF15 protein content was detected by Western Blot analysis, and significant levels of secreted GDF15 were detected by ELISA 48 hours following fenofibrate treatment (***Fig. 8B*** and ***C***, respectively).

SF3B2 and p63RhoGEF are targets of miR-3189-3p

Since GDF15 is strongly upregulated by fenofibrate and miR-3189 is encoded within its intron (**Fig. 7**), we sought to investigate whether the expression of miR-3189 was contributing to the biological function of GDF15. We first determined whether this microRNA is expressed in glioblastoma cells under conditions that are known to upregulate GDF15. If so, we also asked whether this upregulation would be strand-specific to miR-3189-3p, -5p, or both. To answer these questions, LN-229 cells were treated with 50 µM fenofibrate (FF) for 48h followed by qRT-PCR analysis using RNU6B as

the reference gene. ***Fig. 9A*** shows the relative expression of miR-3189-3p and -5p in FF-treated cells as compared to untreated control. Results indicate that the mature microRNAs encoded by miR-3189 are differentially expressed with only miR-3189- 3p expression being strongly induced under pro-apoptosis stimuli. We next tested if miR-3189- 3p was functionally associated to Argonaute 2 (Ago2) complexes by RNA-IP using Ago2 antibody followed by real time PCR (see Materials and Methods). Efficient IP for Ago2 was evaluated by Western blot (***Fig. 9B***). When compared to untreated cells, nearly 35-fold overexpression of miR-3189-3p linked to Ago2 immunocomplexes was measured in extracts from fenofibrate treated cells (***Fig. 9C***). Although not necessarily related to the specific binding to miR-3189-3p, we also measured an increase in SF3B2 and GEFT in the Ago2-IP complexes derived from fenofibrate-treated samples (***Fig. 9D***). Note that, although lower amounts of Ago2 were immunoprecipitated in FF-treated compared to untreated cells (***Fig. 9B***, compare lanes 6 and 8), complexes were still able to efficiently bind miR-3189-3p and its predicted targets SF3B2 and p63RhoGEF mRNAs (***Fig. 9C*** *and* ***D***). In agreement with the detection of SF3B2 and p63RhoGEF mRNAs in the Ago2 complex, we have observed a strong downregulation of SF3B2 mRNA and protein levels in fenofibrate treated cells compared to untreated (***Fig. 10A*** *and* ***C***). Similarly to SF3B2, fenofibrate induced also a downregulation of p63RhoGEF mRNA; however, in this case the effect was significantly less pronounced, and could reflect higher stability of p63RhoGEF mRNA and/or protein in fenofibrate-treated cells (***Fig. 10A*** *and* ***C***). The direct contribution of miR-3189-3p to SF3B2 and p63RhoGEF mRNA and protein levels was evaluated in miR-3189-3p transfected cells by quantitative RT-PCR and Western blot analyses. In comparison to controls, nearly 5-fold and 2.5-fold lower levels of SF3B2 mRNA and p63RhoGEF mRNA were detected in miR-3189-3p expressing cells, respectively (***Fig. 10B***). Importantly, we were able to counteract downregulation of these two transcripts by overexpressing the

anti-miR-3189-3p (miR-3189-3p inhibitor), further supporting the presence of miR-3189-3p-specific regulation. A remarkable down-regulation of SF3B2 and p63RhoGEF at the translational level was confirmed by Western blots in cells transfected with miR-3189-3p, when compared to control or cells co-transfected with the anti-miR- 3189-3p (***Fig. 10D***). There are two putative binding sites for miR-3189-3p in the 3'UTR sequence of SF3B2 mRNA, one conserved (MS2) and one non-conserved (MS1), and their expression was tested by a luciferase-based reporter assay (***Fig. 11A***). A reduction of approximately 75% of luminescence was observed in cells expressing miR-3189-3p, and again this inhibition was almost completely alleviated in the presence of anti-miR-3189-3p. In addition, site directed mutagenesis of the microRNA binding sequences in the 3'UTR showed a slightly different, although cumulative, inhibitory activity. The conserved microRNA binding site (MS2) appeared to be slightly more effective in microRNA-induced transcript degradation as mutation of this site significantly reversed a decrease in luciferase signal (compare MS1 and MS2). As expected, mutation of both microRNA binding sequences (double mutation, DM) abrogated inhibition by miR-3189-3p. In fact, a slight increase in luciferase signal over 3'UTR alone was observed, possibly because mutation of both binding sequences also prevents binding by endogenous miR-3189-3p (***Fig. 11A***). The p63RhoGEF 3'UTR contains three putative binding sites for miR-3189-3p, one conserved and two non-conserved. Similarly to SF3B2 3'UTR, we have tested p63RhoGEF 3'UTR (***Fig. 11B***). Also here, the inhibition was efficiently reverted either in the presence of anti-miR- 3189-3p or by mutating the three binding sequences (triple mutation, TM) of the p63RhoGEF 3'UTR. Quantitatively, one of the non-conserved binding sites did not appear to be required for miR-3189-3p-induced gene regulation, since mutation of this site (MS1) failed to revert the expected inhibition. Conversely, mutation of the other two microRNA binding sites (MS2 and MS3), one conserved and one

non-conserved, showed a stronger and cumulative reversion of inhibition by miR-3189-3p (***Fig. 11B***).

MiR-3189-3p regulates growth and migration of glioblastoma cells

We next evaluated the function of miR-3189-3p in cell growth and migration of the human glioblastoma cell line LN-229. At 48 hours post-transfection morphology of miR-3189-3p expressing cells was visibly altered, presenting a more polygonal shape when compared to the typical spindle-shaped LN-229 cells under normal growth conditions or when both miR-3189-3p and anti-miR-3189-3p were co-expressed (***Fig. 12A***). In addition, the expression of miR-3189-3p resulted in a 50% reduction in cell growth (% decrease in cell number over control; ***Fig. 12B***), accompanied by a significant, 40% reduction in S phase index, as determined by cell cycle distribution analysis (***Fig. 12C***). No significant changes were observed when miR-3189-3p was co-transfected with anti-miR-3189-3p, and the cells expressing this inhibitor behaved essentially as the control, mock-transfected cells. Since miR-3189-3p downregulates also p63RhoGEF mRNA, we evaluated possible effects of this microRNA on cell migration using scratch assay and by monitoring both cell locomotion and cell division using time-lapse imaging. While control cells populated the entire scratched area in 18 hours, the cells transfected with miR-3189-3p covered only 42% of the scratched surface (***Fig. 12D***) in the same amount of time. Both decreased cell motility and decreased cell proliferation contributed to the observed attenuation of the invasion of the cell-free space.

Role of SF3B2 and p63RhoGEF to the inhibition of cellular growth and migration induced by miR-3189-3p

Since SF3B2 expression is strongly downregulated by miR-3189-3p, we hypothesized that forced expression of SF3B2 might reverse the miRNA -mediated effects on cell proliferation. Results from growth rate analysis in ***Figure 13A*** provide evidence, which confirms this assumption *(**Fig. 13***). Moreover, we measured that constitutive expression of SF3B2 was enough to rescue cell growth to steady-state levels despite addition of miR-3189-3p. Conversely, downregulation of SF3B2 by siRNA mimics the biological effects of miR-3189-3p expression by inducing 55% reduction in cell growth (***Fig. 13B***). The impaired growth by SF3B2 is likely mediated by E2F-1, a known molecule downstream of SF3B2 that is important for cell cycle progression [177]. The Western blot in ***Fig. 13C*** shows marked down-regulation of E2F-1 protein levels in LN-229 cells transfected with miR-3189-3p and this effect was reversed in the presence of the anti-miR-3189-3p. Therefore, these data suggest that E2F-1 is a potential downstream target of miR-3189-3p/SF3B2 in coordinating delayed cell growth in our model.

Next, we evaluated the contribution of p63RhoGEF to the inhibitory effects of miR-3189-3p expression on cell migration. Silencing p63RhoGEF in LN-229 resulted in 54% (± 7%) inhibition of migration (***Fig. 14A***) confirming previously reported data [183]. To test the contribution of p63RhoGEF on the inhibition of migration due to miR-3189-3p we generated a stable cell line over-expressing p63RhoGEF and we utilized two clones that showed different expression levels of the protein (***Fig. 14B***, inset). When tested using the scratch assay, both clones of the p63RhoGEF-expressing cells behaved essentially as the control cells (transfected with pcDNA3.1 empty vector), however transient transfection with the miR-3189-3p was still capable of reducing cell migration by 60% (***Fig. 14B***). Altogether, those results indicate that downregulation of SF3B2 by miR-3189-3p is necessary

and sufficient for the miR-mediated impairment of cell growth, while down-regulation of p63RhoGEF might be required but is not sufficient for the inhibition of migration by miR-3189-3p.

MiR-3189-3p is downregulated in human brain tumors and has tumor suppressor activity in mice

Next, the ability of miR-3189-3p to inhibit tumor growth was evaluated *in vivo*. LN-229 cells, bearing the pmCherry plasmid to facilitate detection of the tumor by fluorescence, were mock-transfected or transfected with miR-3189-3p mimic. Next day, $2x10^6$ of either cell line were injected subcutaneously in the flank of nude mice (n=5 per group). Beginning at one week post-injection, mice were visualized via *in vivo* biophotonic epifluorescence and the mean fluorescence radiance for each tumor was collected. We found that mice bearing LN-229/miR-3189-3p cells had a nearly 75% smaller tumors when compared to LN-229/Mock (***Fig.15, A*** and ***B***; $p<0.05$). The same results were observed in nude mice bearing subcutaneous injection of U87MG-luciferase/miR-3189-3p cells in comparison to U87MG-luciferase/Mock cells (data not shown). Moreover, the anti-tumor growth effect of miR-3189-3p was also confirmed in nude mice bearing intracranial U87MG glioblastoma cells mock-transfected or transfected with miR-3189-3p mimic (***Fig.15***, ***C*** and ***D***). Beginning at one week post-injection, the mean luminescence radiance for each tumor was collected. After two weeks we found that mice bearing U87MG/miR-3189-3p cells had a nearly 72% smaller tumors when compared to U87MG/Mock (***Fig.15, C*** and ***D***; $p<0.0005$).

Since GDF15 and miR-3189 originate from the same transcript, we asked whether their expression would correlate with that measured in human brain tumor extracts. Frozen tissue samples from astrocytomas, glioblastomas and normal brains were utilized for total RNA isolation and were subjected to

quantitative RT-PCR. Results shown in ***Fig. 16A*** and **B** represent the relative expression (1/ΔCt) of the indicated RNA species normalized using RNU6B as reference gene. Interestingly, although GDF15 was not detected by real time PCR in normal brain tissues, its expression yielded a trend specific to tumor type with higher upregulation in glioblastoma than in astrocytomas (***Fig. 16A***; $p<0.05$). Conversely, miR-3189-3p levels were significantly lower in both astrocytomas and glioblastomas compared to control brain tissue ($p<0.05$ and $p<0.001$, respectively), and showed a trend that correlated with the tumor progression (***Fig. 16B***). Of the two major targets of miR-3189-3p, SF3B2 and p63RhoGEF, only SF3B2 showed a statistically significant increased in expression in both astrocytomas and glioblastomas compared to the control group ($p<0.01$ and $p<0.05$, respectively), ***Fig. 16C***, while p63RhoGEF mRNA expression analysis did not result in significant changes between the three groups (***Fig. 16D***).

GDF15 and miR-3189-3p expression upon fenofibrate stimulation is PPARα-independent

Next, we wanted to investigate the transcriptional factors that can be potentially involved in the fenofibrate-induced up-regulation of GDF15 and miR-3189-3p, with particular regard to PPARα, the receptor by which fenofibrate exerts its effects.

As mentioned above, several studies have shown also PPARα-independent activities of fenofibrate [152,154,159,169]. In detail, in a work of 2009 Araki and colleagues, by analyzing microarray data of human endothelial cells treated with fenofibrate and with or without siRNA against PPARα, suggest that GDF15 is a PPARα-independent master regulator of fenofibrate action [159,169]. Here, we showed that both GDF15 and miR-3189-3p up-regulation observed upon fenofibrate stimulation is PPARα-independent as demonstrated by treating LN-229 with PPARα inhibitor (***Fig.***

17A) and by transfection assay with siRNA against PPARα (***Fig. 17B***). PPARα mRNA expression level was effectively downregulated by siRNA against PPARα but was not affected by scrambled siRNA. Results are expressed as fold change ($2^{-\Delta\Delta Ct}$ method) of the mRNA in siRNA scramble and siRNA PPARα transfected LN-229 cells compared to control (untransfected, MOCK).

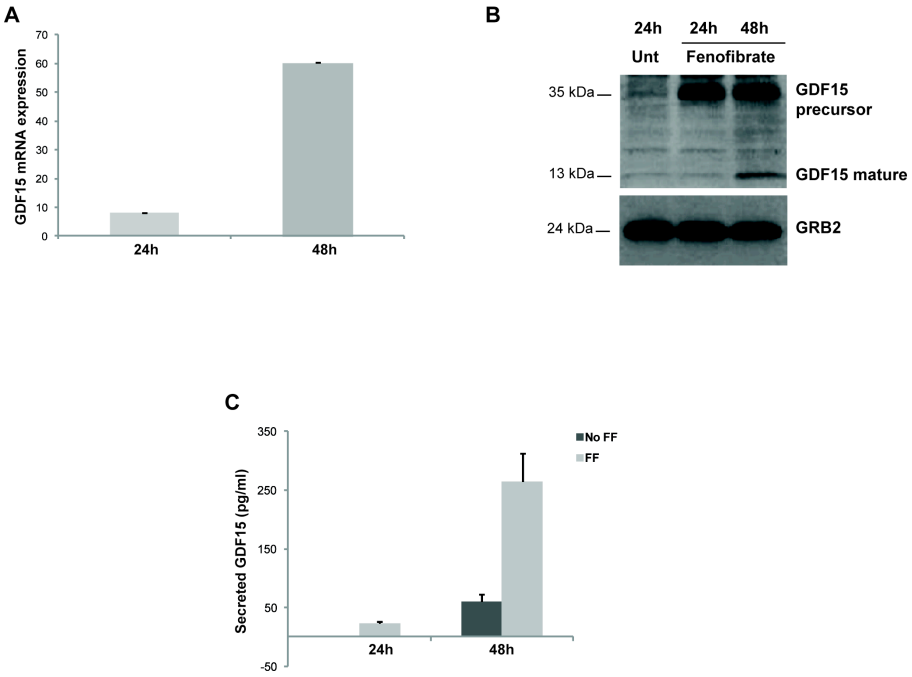

Figure 8: Fenofibrate treatment up-regulates GDF15 mRNA and protein expression in LN-229 cells.

***A**, Real-time PCR detecting GDF15 mRNA expression at the indicated time points after fenofibrate treatment. Results are expressed as fold change ($2^{-\Delta\Delta Ct}$ method) of the mRNA in fenofibrate-treated LN-229 cells compared to untreated. In the same experimental conditions, mature and precursor GDF15 proteins were detected by Western blots (**B**). Grb2 antibody was used to show equal loading of cellular lysates. **C**, ELISA to detect secreted mature (active) GDF15 protein in the culturing medium obtained from LN-229 cells treated with fenofibrate (FF) and control (no FF). The data represent change in GDF15 levels in medium from fenofibrate-treated cells compared to untreated.*

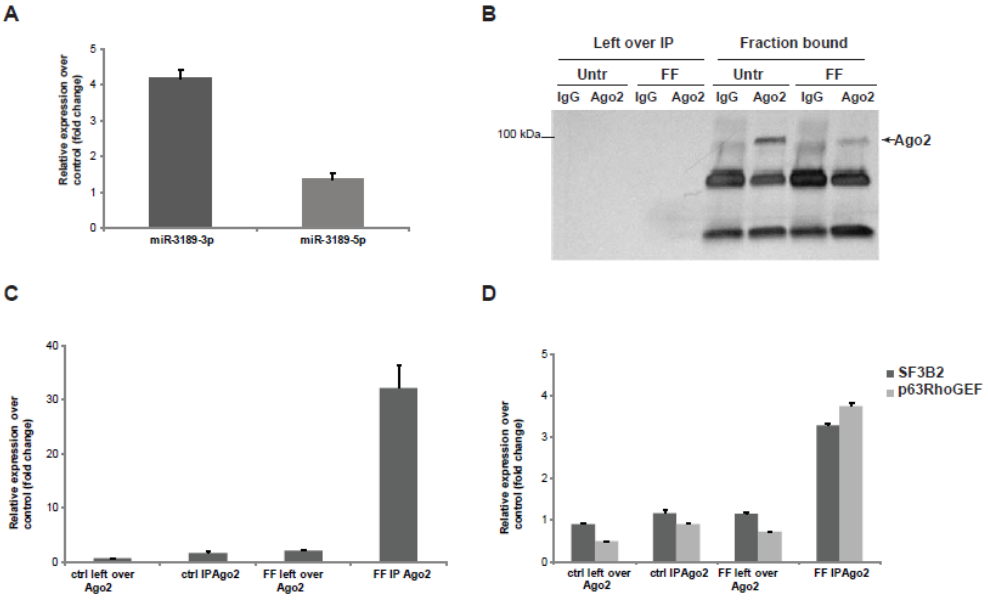

Figure 9: MiR-3189-3p is upregulated and incorporated into the RNA-induced silencing complex (RISC) in cells treated with fenofibrate.

***A**, Real-time PCR to detect miR-3189-3p and miR-3189-5p expression. Results are expressed as fold change of the microRNAs in fenofibrate-treated cells (FF) compared to untreated. **B**, Western Blot to detect Ago2 after immunoprecipitation of lysates obtained from untreated and fenofibrate-treated cells. Left over IP represents the fraction of lysates obtained after overnight incubation with Ago2 antibody or the control isotype IgG, and used as negative control. **C** and **D**, Real-time PCR detection of miR-3189-3p (**C**) and targets (**D**), SF3B2 and p63RhoGEF, incorporation into Ago2 following treatment with fenofibrate. The enrichment of microRNAs in RISC was calculated according to the formula $2^{-(CtAgo2 - CtIgG)}$ and normalized over RNU6B for microRNAs and GAPDH for mRNA.*

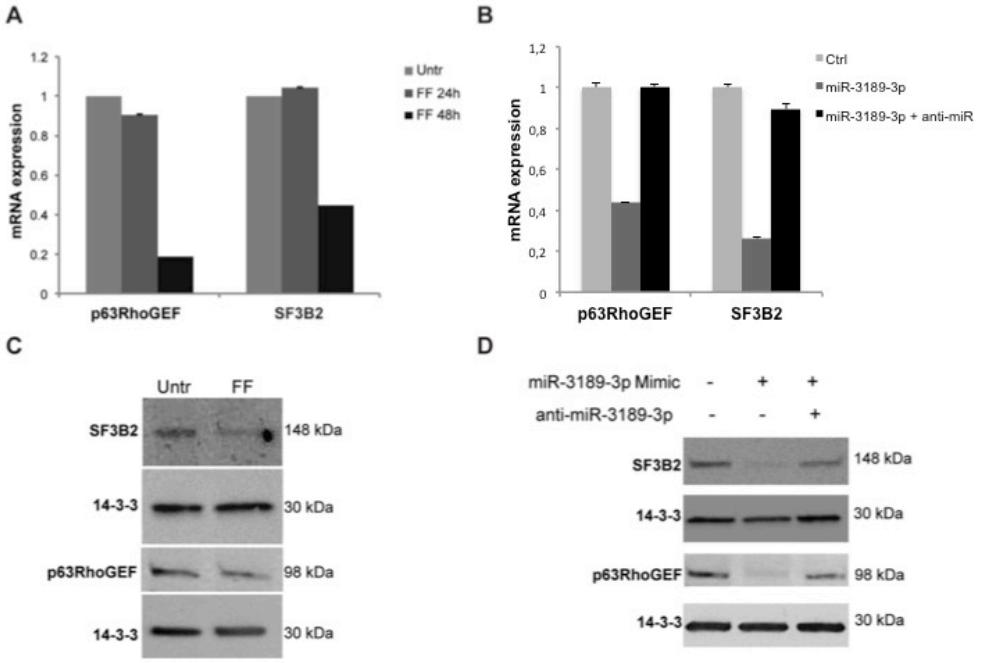

Figure 10: Fenofibrate treatment results in down-regulation of miR-3189-3p target mRNAs and proteins in LN-229 cells.

***A**, Real-time PCR data showing changes in p63RhoGEF and SF3B2 mRNAs after fenofibrate treatment for 24 and 48 hours. Results are expressed as fold change of the mRNA in fenofibrate-treated cells compared to the untreated (Untr). **B**, Real-time PCR showing expression of p63RhoGEF and SF3B2 mRNAs in mock-transfected (Ctrl), cells transfected with miR-3189-3p, and cells transfected with miR-3189-3p + anti-miR-3189-3p. Results are expressed as fold change compared to mock-treated cells. **C**, Western blots for SF3B2 and p63RhoGEF proteins performed on lysates from cells that were untreated or treated with fenofibrate (FF) for 48 hours. 14-3-3 antibody was used to show equal loading of cellular lysates. **D**, Western blots for SF3B2 and p63RhoGEF proteins performed on lysates from cells transfected with mock, miR-3189-3p, or miR-3189-3p + anti-miR-3189-3p for 48 hours.*

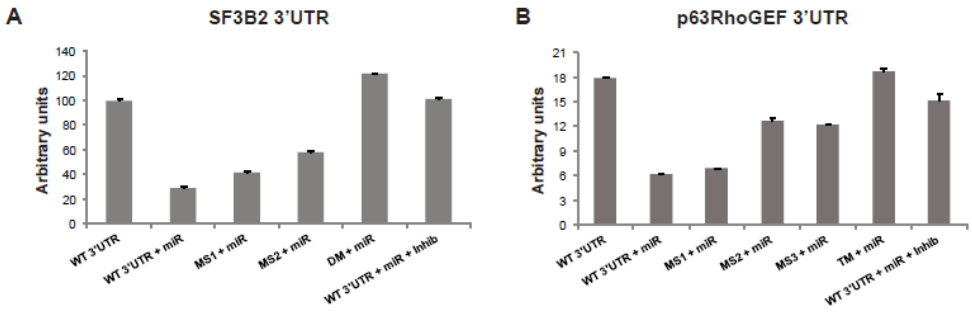

Figure 11: MiR-3189-3p directly targets the 3'UTR sequences of SF3B2 and p63RhoGEF.

A, *Luciferase assays of LN-229 cells co-transfected with psiCHECK2/SF3B2 3'UTR and the mutants in the miR-3189-3p putative binding sites (MS1 and MS2) and miR-3189-3p +/- anti-miR-3189-3p (inhib).* ***B***, *Luciferase assays of LN-229 cells co-transfected with spiCHECK2/p63RhoGEF 3'UTR and mutants (MS1, MS2, MS3) and miR-3189-3p +/- anti-miR-3189-3p (inhib). Lucifarese and Renilla values were determined at 24 hours post-transfection. The data represent the ratio between Renilla Luciferase values and Firefly Lucifarese internal control for each group (n = 2). MS1-3 indicate specific microRNA binding site mutants; DM and TM indicate double- and triple-binding site mutants.*

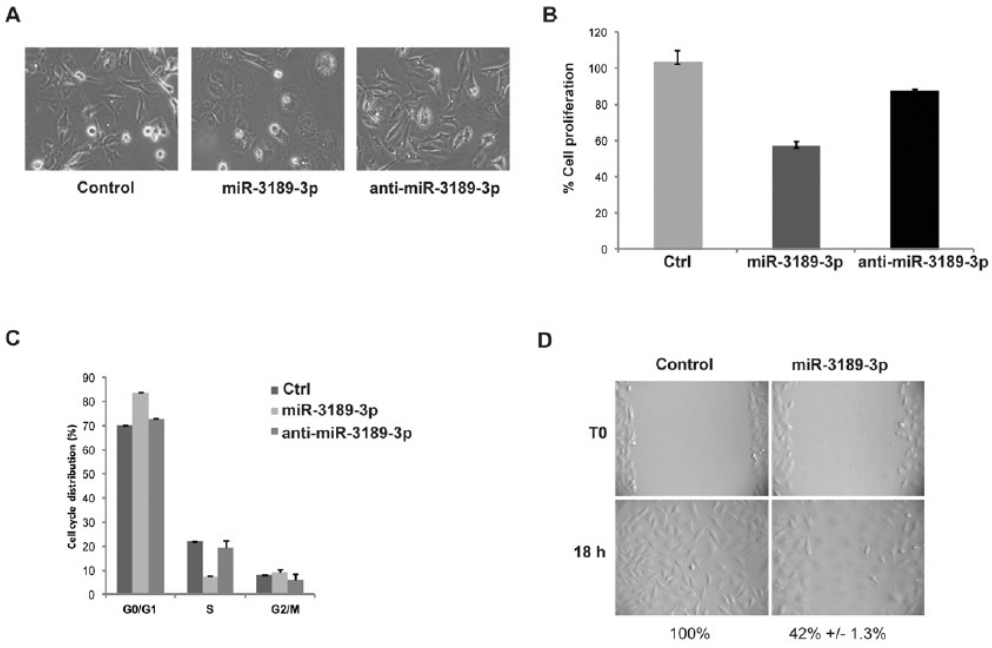

Figure 12: MiR-3189-3p alters the morphology and impairs the growth and migration of LN-229 gioblastoma cells.

***A**, Phase contrast images showing the morphology of LN-229 cells following trasnfection with miR-3189-3p or miR-3189-3p + anti-miR-3189-3p; original magnification 10X. Images were acquired at 48 hours post-transfection. **B**, Cell-growth assay performed 72 hours post-transfection with mock (Ctrl), miR-3189-3p or miR-3189-3p + anti-miR-3189-3p and quatified using MTS reagent. Results are expressed as percent growth/mock-treated control. **C**, Cell cycle analysis of LN-229 cells transfected with mock (Ctrl), miR-3189-3p and miR-3189-3p + anti-miR-3189-3p. Cells were stained with Guava Cell Cycle reagent and cell cycle distribution (%) was quantified by flow cytometry using FACSAria. **D**, Representative images of a scratch assay to monitor migration of controls (mock transfected) and miR-3189-3p transfected cells; original magnification 10X. Migration into the cell-free area was monitored by time-lapse imaging in a VivaView incubator.*

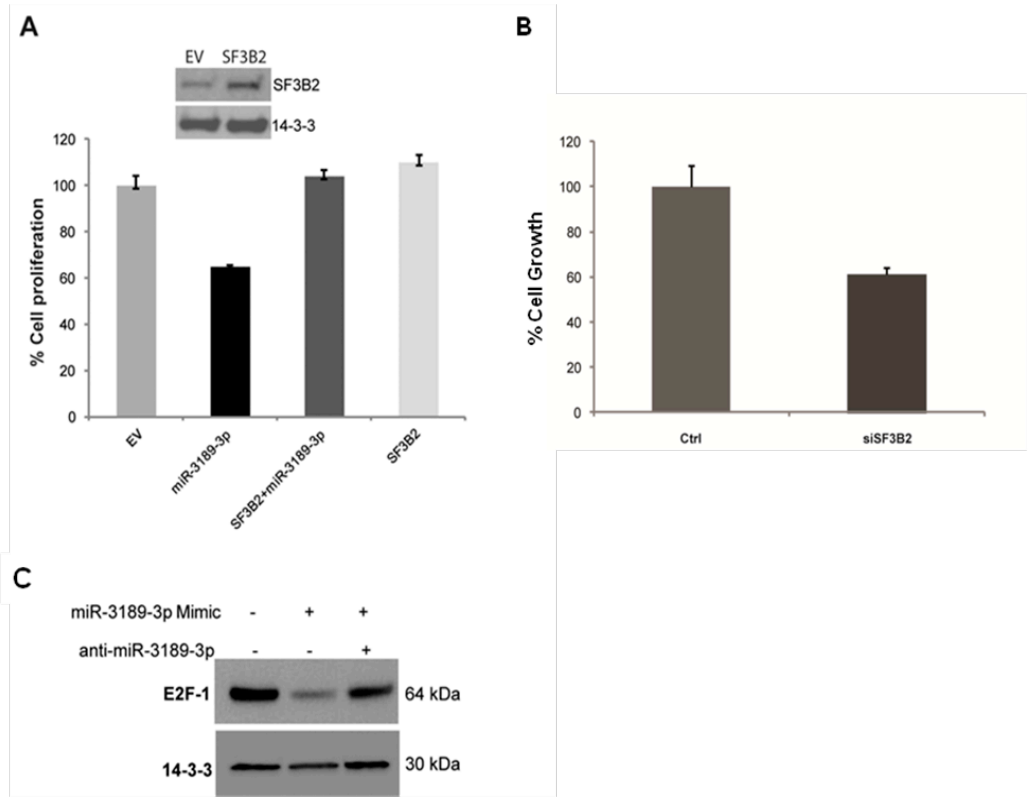

Figure 13: MiR-3189-3p regulates LN-229 cell growth through the down-regulation of SF3B2.

***A**, Cell growth assay performed 72 hours after transient transfection of LN-229/pcDNA3.1 (empty vector, EV) or LN-229/SF3B2 with miR-3189-3p. The inset shows levels of expression of SF3B2 in the stably transfected cells. Results are expressed as percent growth/mock-treated control. **B**, Cell growth assay performed 48 hours after transient transfection of siSF3B2. **C**, Western blots for E2F-1 protein expression performed on lysates from cells transfected with mock, miR-3189-3p, or miR-3189-3p + anti-miR-3189-3p. 14-3-3 antibody was used to show equal loading of cellular lysates.*

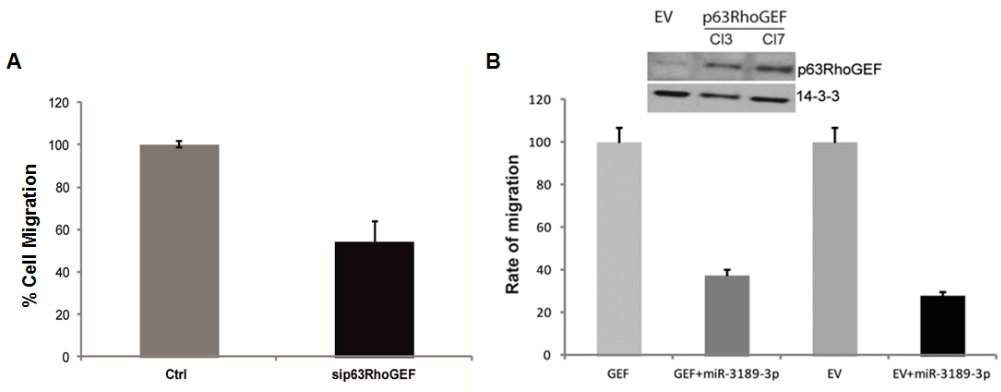

Figure 14: MiR-3189-3p regulates LN-229 cell migration through the down-regulation of p63RhoGEF.

***A**, Cell migration assay performed 48h after transient transfection of sip63RhoGEF.* ***B**, Diagram showing the results of a scratch assay to monitor migration of cells stably expressing the p63RhoGEF gene (GEF). Migration into cell-free area was monitored by time-lapse imaging in a VivaView incubator. The inset shows levels of expression of p63RhoGEF protein in two clones of the stably transfected LN-229 cells and control empty vector (EV).*

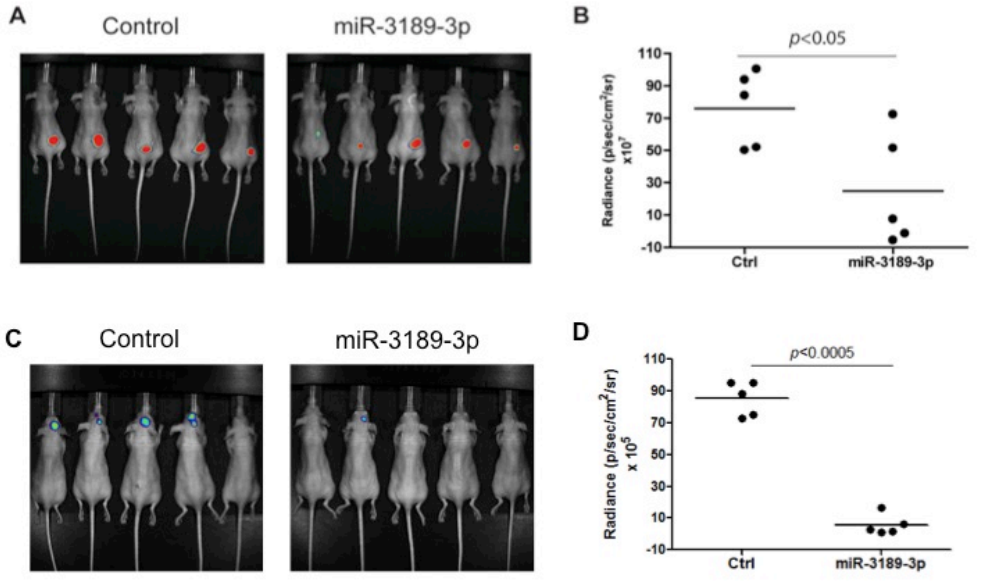

Figure 15: Expression of miR-3189-3p results in growth inhibition of human glioblastoma cells in mice.

***A**, Fluorescent images of pmCherry/LN-229 cells mock-transfected (Control) or transfected with miR-3189-3p implanted subcutaneously in nude mice ($p<0.05$). **B**, Plot of tumor burden 3 weeks post-injection with control or miR-3189-3p-transfected LN-229-mCherry cells. Tumor burden was quantified by acquiring fluorescent emission at 610 nm wavelength. Relative fluorescence values are represented as photon flux per second, square centimeter and surface radiance (p/sec/cm^2/sr). **C**, Luminescent images of U87MG-luciferase cells mock-transfected (Control) or transfected with miR-3189-3p implanted intracranially in nude mice ($p<0.0005$). **D**, Plot of tumor burden 2 weeks post-injection with control or miR-3189-3p-transfected U87MG-luciferase cells. Tumor burden was quantified by acquiring luminescence emission. Relative luminescence values are represented as photon flux per second, square centimeter and surface radiance (p/sec/cm^2/sr).*

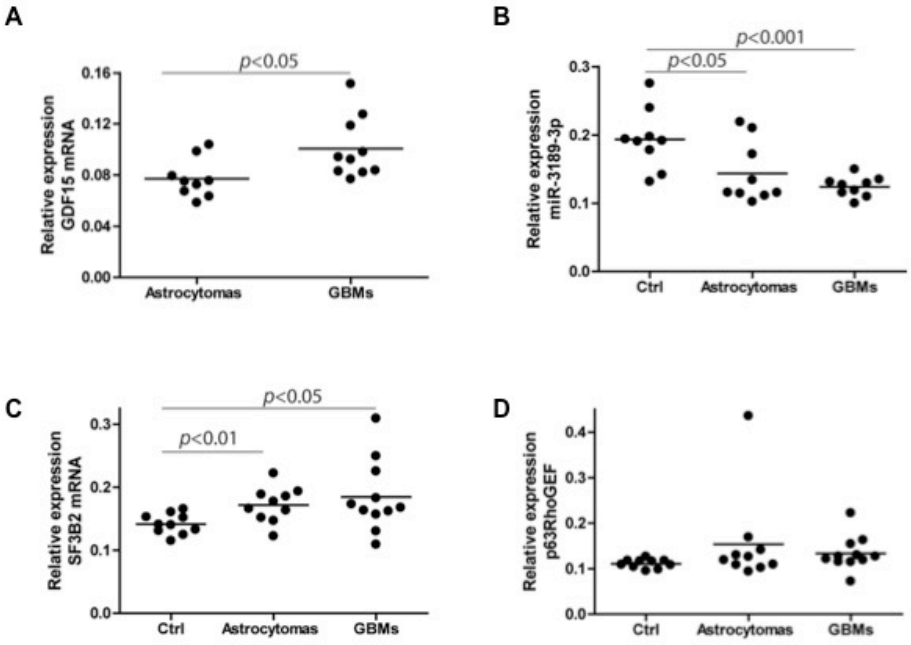

Figure 16: Expression of miR-3189-3p inversely correlates with tumor grade and SF3B2 and p63RhoGEF expression in human clinical samples.
A*, Relative expression of GDF15 mRNA in human astrocytoma and glioblastoma clinical samples, calculated as 1/ΔCt. Note that GDF15 mRNA was undetectable in control brain samples.* ***B*** *–* ***D****, Relative expression of miR-3189-3p, SF3B2, and p63RhoGEF mRNA in normal control (Ctrl), astrocytoma, or glioblastoma clinical samples. Results are expressed as 1/ΔCt values. T-test results (p-values) are shown in the graphs.*

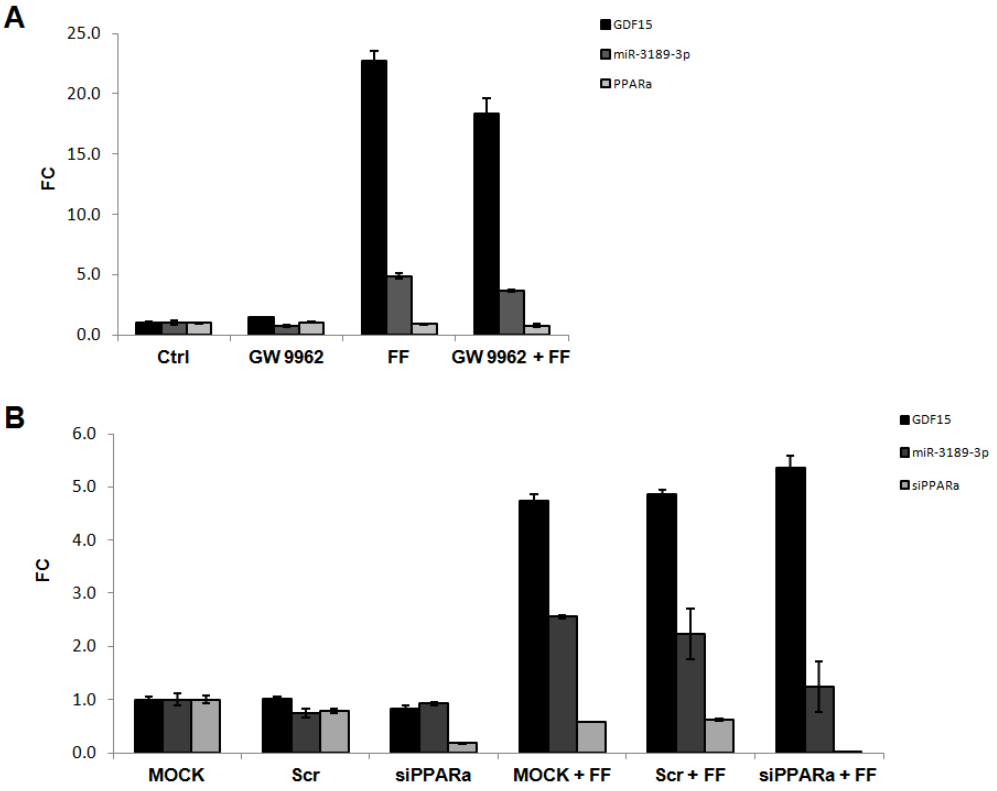

Figure 17: Expression of GDF15 and miR-3189-3p upon fenofibrate stimulation is PPARα-independent.

***A**, Real-time PCR detecting GDF15 mRNA, PPARα mRNA and miR-3189-3p expression in fenofibrate-treated LN-229 at 48 hours time-point with or without PPARα-inhibitor (GW 9962). Results are expressed as fold change ($2^{-\Delta\Delta Ct}$ method) of the mRNA or of the microRNA in fenofibrate-treated LN-229 +/- GW 9962 compared to untreated (Ctrl). **B**, Real-time PCR detecting GDF15 mRNA, PPARα mRNA and miR-3189-3p expression at 48 hours time-point after transfection. LN-229 cells were incubated with 100 nM of siRNA against human PPARα or 100 nM scrambled siRNA.*

DISCUSSION

GDF15 is a secreted protein that plays a central role in diverse biological processes including differentiation, proliferation, apoptosis, and regulation of the inflammatory response [123]. In cancer, there are contradictory reports on the tumor promoting and tumor suppressive properties of GDF15. For instance, increased expression of GDF15 has been observed during the progression of several aggressive cancers, such as melanoma, colorectal, prostate, pancreatic, breast and brain. Conversely, cytotoxic agents such as etoposide and doxorubicin have been shown to increase GDF15 expression [123]

MiR-3189 has been previously predicted to be a mirtron expressed in melanoma [185] but no experimental evidence has been demonstrated so far. An inhibitory effect of miR-3189-5p on TGFβR2 has been hypothesized [186], but a function for neither miR-3189-3p nor miR-3189-5p has been identified. Mirtrons are microRNAs encoded within introns and their biogenesis follows a non-canonical, Drosha/DGCR8-independent, pathway that relies on the mRNA splicing and on RNA lariats debranching enzymes [31]. Differently from canonical pre-miRNA stem-loops, microRNAs generated from the 3' (-3p) of the mirtron hairpin appear to be more stable than those generated from the 5' (-5p) [187]. This may explain why, even if miR-3189-5p expression was slightly and variably induced by mitogenic stimuli (10% FBS), the microRNA was not detected in the Ago2-immunoprecipitated complex (data not shown).

MiR-3189-3p together with two of its major predicted targets, SF3B2 and p63RhoGEF, co-immunoprecipitated with Ago2 (***Fig. 9****),* suggesting a functional role for this microRNA. A direct inhibitory effect of miR-3189-3p on the 3' UTR sequence of SF3B2 and p63RhoGEF was further demonstrated by luciferase assay (***Fig. 11***). Fenofibrate treatment and over-expression of miR_3189-3p in LN-229 cells also resulted in down-regulation of SF3B2 and p63RhoGEF (***Fig. 10***). However the presence of antago-miR against miR-3189-3p in fenofibrate-treated cells did not rescue SF3B2 or p63RhoGEF

expression or protect cells from apoptosis (data not shown). Given the broad range of effects triggered by fenofibrate [152,156,166] it is possible that changes in microRNA expression may only partially contribute to its biological function. Nevertheless, expression of miR-3189-3p had a strong biological effect on LN-229, impairing their migration and growth. These effects were shown being mediated through downregulation of p63RhoGEF and SF3B2, respectively (***Fig. 13*** and ***14***). With respect to p63RhoGEF previous reports have also shown a role for this protein in cell migration. Specifically, Hayashi et al. demonstrated that the expression of p63RhoGEF is essential for lamellipodial polarization during serum-induced chemotaxis [183]. Our findings are in agreement with a role for p63RhoGEF in cell motility, since siRNA against p63RhoGEF impaired migration of LN-229 cells (***Fig. 14A***). Our results showing the inhibitory effect of miR-3189-3p on p63RhoGEF overexpressing cells (***Fig. 14B***), demonstrate that inhibition of cell migration by miR-3189-3p is only partially due to the downregulation of p63RhoGEF. Such result may not be surprising, since other members of the RhoA family of guanine nucleotide exchange factors, as SLIT-ROBO Rho GTPase activating protein 2 (SRGAP2) and Rho guanine nucleotide exchange factor (GEF) 12 (ARHGEF12) are other putative targets of miR-3189-3p. Likewise, the striking change in cellular morphology upon expression of miR-3189-3p might be the result of this microRNA targeting multiple genes involved in cytoskeletal remodeling.

It has been reported that the expression of the transcription factor E2F-1 is dependent on the presence of SF3B2 in the cell [177]. Furthermore, E2F-1 has been shown to be a master regulator of cell cycle progression [188,189]. Therefore, it is not surprising that SF3B2 downregulation by miR-3189-3p in glioblastoma delayed cell growth. In our studies, this effect was shown to be dependent on SF3B2, as overexpression of this gene in the presence of miR-3189-3p restored the proliferative capacity of LN-229 cells. The antiproliferative activity of miR-3189-3p was also demonstrated *in vivo*

both in nude mice bearing subcutaneous LN-229 tumors (***Fig. 15A*** and ***15B***) and in nude mice bearing subcutaneous U87MG tumors. Finally, results obtained from nude mice bearing intracranial U87MG tumors confirmed the antiproliferative activity of miR-3189-3p (***Fig. 15B*** *and* ***15D***).

Importantly, miR-3189-3p and its targets SF3B2 and p63RhoGEF, along with GDF15 were differentially expressed in clinical samples of glial tumors. GDF15 mRNA was not detected in normal brain tissue, but its transcripts were significantly increased in glioblastomas compared to astrocytomas (***Fig. 16A***). Expression levels of miR-3189-3p and its target SF3B2 were inversely correlated, as the microRNA was downregulated and SF3B2 mRNA was upregulated in astrocytomas and glioblstomas when compared to normal tissue (***Fig. 16***, panels ***B*** and ***C***). Although expression of p63RhoGEF mRNA may indicate a trend in increased levels in both glial tumors when compared to controls, the difference was not statistically significant (***Fig. 16D***). Overexpression of GDF15 protein or treatment of LN-229 cells with its soluble version did not elicit any morphological or biological effects in LN-229 cells *in vitro* (data not shown). Similarly, the anti-miR-3189-3p did not protect fenofibrate-treated cells from apoptosis, indicating that upregulation of miR-3189-3p is not required for fenofibrate-mediated cell death. Nevertheless, our study shows that expression of GDF15 and its co-encoded miR-3189-3p is regulated in brain tumors, and that miR-3189-3p acts as a tumor suppressor.

CONCLUSIONS

In this study, we have analyzed the role of GDF15 and its co-encoded miR-3189 in glioblastoma. In particular we focused on the characterization of the function of miR-3189-3p, which we found to be interestingly upregulated together with GDF15 after fenofibrate treatment in LN-229 cells. Numerous published works demonstrate the anticancer properties of fenofibrate, while contradictory evidences exist about the tumor-promoting or the tumor-suppressive role of GDF15. Moreover, the functions for neither miR-3189-3p nor miR-3189-5p have been identified so far. Thus this is the first report where the role of these two microRNAs, and in particular miR-3189-3p, has been investigated in order to study their possible participation in the biological function of GDF15.

Results presented herein indicate that miR-3189-3p has a tumor-suppressor function by acting on two of its major predicted targets, SF3B2 and p63RhoGEF, involved respectively in cell-proliferation and cell-migration. Indeed transfection of LN-229 cells with miR-3189-3p resulted in a delayed cell-growth and in a slowdown of migration. The validation of the targeting on these two genes was conducted by performing both Luciferase assays and Ago2 immunoprecipitation. Luciferase assays demonstrated the downregulation of SF3B2 and p63RhoGEF through the binding of miR-3189-3p to their 3'UTR. Ago-2 immunoprecipitation experiments upon fenofibrate stimulation showed an enrichment of miR-3189-3p together with SF3B2 and p63RhoGEF in Ago-2 complexes, suggesting that miR-3189-3p was functionally associated with Ago-2. In addition, both the subcutaneous and the intracranial injection in mice of cell-lines bearing the miR-3189-3p resulted in inhibition of tumor growth, strongly validating the antiproliferative activity of this microRNA. Importantly, the tumor-suppressor activity of miR-3189-3p has been confirmed by conducting the major experiments in other glioblastoma cell-lines (U87MG, T98G), corroborating the potential clinical implication of our findings.

Analyses on clinical specimens of brain tumors revealed that miR-3189-3p is under-expressed in astrocytoma and glioblastoma samples, showing an opposite trend compared to its targets, which is in agreement with the results obtained *in vitro* validating its role as a tumor-suppressor. Moreover, the opposite trend observed in clinical samples between GDF15 and miR-3189-3p may explain its effect in the biological function of GDF15 that is its contribution to determine the oncogenic role of the protein in the late stages of the tumor progression.

Altogether, our studies have demonstrated that miR-3189-3p controls the growth and migration of glioblastoma cells by targeting the SF3B2 and p63RhoGEF mRNAs. Importantly, drugs, such as fenofibrate, that increase miR-3189-3p expression have the potential of slowing down glioblastoma growth and central nervous system (CNS) invasion. For instance we have found that stimulating LN-229 with other treatments besides fenofibrate, such as Carnosic Acid and N-acetylsalicylic Acid (data not shown), are able to induce an up-regulation of both GDF15 mRNA and miR-3189-3p expression.

Further studies on the biological activity of this microRNA using glioblastoma as a model may help the development of new supplemental anti-cancer therapy supporting both the existing and emerging anti-glioblastoma treatments.

BIBLIOGRAPHY

1. Mattick JS, Makunin IV (2006) Non-coding RNA. Hum Mol Genet 15 Spec No 1: R17-29.
2. Mattick JS (2001) Non-coding RNAs: the architects of eukaryotic complexity. EMBO Rep 2: 986-991.
3. International Human Genome Sequencing Consortium (2004) Finishing the euchromatic sequence of the human genome. Nature 431: 931-945.
4. Calore F, Lovat F, Garofalo M (2013) Non-coding RNAs and cancer. Int J Mol Sci 14: 17085-17110.
5. Da Sacco L, Baldassarre A, Masotti A (2012) Bioinformatics tools and novel challenges in long non-coding RNAs (lncRNAs) functional analysis. Int J Mol Sci 13: 97-114.
6. Lee RC, Feinbaum RL, Ambros V (1993) The C. elegans heterochronic gene lin-4 encodes small RNAs with antisense complementarity to lin-14. Cell 75: 843-854.
7. Wightman B, Ha I, Ruvkun G (1993) Posttranscriptional regulation of the heterochronic gene lin-14 by lin-4 mediates temporal pattern formation in C. elegans. Cell 75: 855-862.
8. Cullen BR (2004) Transcription and processing of human microRNA precursors. Mol Cell 16: 861-865.
9. Di Leva G, Garofalo M, Croce CM (2014) MicroRNAs in cancer. Annu Rev Pathol 9: 287-314.
10. Kozomara A, Griffiths-Jones S (2011) miRBase: integrating microRNA annotation and deep-sequencing data. Nucleic Acids Res 39: D152-157.
11. Bartel DP (2004) MicroRNAs: genomics, biogenesis, mechanism, and function. Cell 116: 281-297.

12. Rom S, Rom I, Passiatore G, Pacifici M, Radhakrishnan S, et al. (2010) CCL8/MCP-2 is a target for mir-146a in HIV-1-infected human microglial cells. Faseb J 24: 2292-2300.
13. Iorio MV, Croce CM (2012) microRNA involvement in human cancer. Carcinogenesis 33: 1126-1133.
14. Olena AF, Patton JG (2010) Genomic organization of microRNAs. J Cell Physiol 222: 540-545.
15. Bartel DP (2009) MicroRNAs: target recognition and regulatory functions. Cell 136: 215-233.
16. Ha M, Kim VN (2014) Regulation of microRNA biogenesis. Nat Rev Mol Cell Biol 15: 509-524.
17. Griffiths-Jones S, Grocock RJ, van Dongen S, Bateman A, Enright AJ (2006) miRBase: microRNA sequences, targets and gene nomenclature. Nucleic Acids Res 34: D140-144.
18. Babiarz JE, Ruby JG, Wang Y, Bartel DP, Blelloch R (2008) Mouse ES cells express endogenous shRNAs, siRNAs, and other Microprocessor-independent, Dicer-dependent small RNAs. Genes Dev 22: 2773-2785.
19. Lee Y, Kim M, Han J, Yeom KH, Lee S, et al. (2004) MicroRNA genes are transcribed by RNA polymerase II. Embo J 23: 4051-4060.
20. Lee Y, Jeon K, Lee JT, Kim S, Kim VN (2002) MicroRNA maturation: stepwise processing and subcellular localization. Embo J 21: 4663-4670.
21. Han J, Lee Y, Yeom KH, Kim YK, Jin H, et al. (2004) The Drosha-DGCR8 complex in primary microRNA processing. Genes Dev 18: 3016-3027.
22. Yi R, Qin Y, Macara IG, Cullen BR (2003) Exportin-5 mediates the nuclear export of pre-microRNAs and short hairpin RNAs. Genes Dev 17: 3011-3016.

23. Zeng Y, Cullen BR (2004) Structural requirements for pre-microRNA binding and nuclear export by Exportin 5. Nucleic Acids Res 32: 4776-4785.
24. Gwizdek C, Ossareh-Nazari B, Brownawell AM, Doglio A, Bertrand E, et al. (2003) Exportin-5 mediates nuclear export of minihelix-containing RNAs. J Biol Chem 278: 5505-5508.
25. Chu CY, Rana TM (2007) Small RNAs: regulators and guardians of the genome. J Cell Physiol 213: 412-419.
26. Meijer HA, Smith EM, Bushell M (2014) Regulation of miRNA strand selection: follow the leader? Biochem Soc Trans 42: 1135-1140.
27. Kim VN (2005) MicroRNA biogenesis: coordinated cropping and dicing. Nat Rev Mol Cell Biol 6: 376-385.
28. Kim VN, Han J, Siomi MC (2009) Biogenesis of small RNAs in animals. Nat Rev Mol Cell Biol 10: 126-139.
29. Gredell JA, Dittmer MJ, Wu M, Chan C, Walton SP (2010) Recognition of siRNA asymmetry by TAR RNA binding protein. Biochemistry 49: 3148-3155.
30. Meister G (2013) Argonaute proteins: functional insights and emerging roles. Nat Rev Genet 14: 447-459.
31. Ruby JG, Jan CH, Bartel DP (2007) Intronic microRNA precursors that bypass Drosha processing. Nature 448: 83-86.
32. Westholm JO, Lai EC (2011) Mirtrons: microRNA biogenesis via splicing. Biochimie 93: 1897-1904.
33. Flynt AS, Greimann JC, Chung WJ, Lima CD, Lai EC (2010) MicroRNA biogenesis via splicing and exosome-mediated trimming in Drosophila. Mol Cell 38: 900-907.
34. Curtis HJ, Sibley CR, Wood MJ (2012) Mirtrons, an emerging class of atypical miRNA. Wiley Interdiscip Rev RNA 3: 617-632.

35. Glazov EA, Kongsuwan K, Assavalapsakul W, Horwood PF, Mitter N, et al. (2009) Repertoire of bovine miRNA and miRNA-like small regulatory RNAs expressed upon viral infection. PLoS One 4: e6349.
36. Chiang HR, Schoenfeld LW, Ruby JG, Auyeung VC, Spies N, et al. (2010) Mammalian microRNAs: experimental evaluation of novel and previously annotated genes. Genes Dev 24: 992-1009.
37. Carthew RW, Sontheimer EJ (2009) Origins and Mechanisms of miRNAs and siRNAs. Cell 136: 642-655.
38. Cifuentes D, Xue H, Taylor DW, Patnode H, Mishima Y, et al. (2010) A novel miRNA processing pathway independent of Dicer requires Argonaute2 catalytic activity. Science 328: 1694-1698.
39. Cheloufi S, Dos Santos CO, Chong MM, Hannon GJ (2010) A dicer-independent miRNA biogenesis pathway that requires Ago catalysis. Nature 465: 584-589.
40. Liu YP, Schopman NC, Berkhout B (2013) Dicer-independent processing of short hairpin RNAs. Nucleic Acids Res 41: 3723-3733.
41. Liu C, Mallick B, Long D, Rennie WA, Wolenc A, et al. (2013) CLIP-based prediction of mammalian microRNA binding sites. Nucleic Acids Res 41: e138.
42. Sheth U, Parker R (2003) Decapping and decay of messenger RNA occur in cytoplasmic processing bodies. Science 300: 805-808.
43. Chan SP, Slack FJ (2006) microRNA-mediated silencing inside P-bodies. RNA Biol 3: 97-100.
44. Liu J, Rivas FV, Wohlschlegel J, Yates JR, 3rd, Parker R, et al. (2005) A role for the P-body component GW182 in microRNA function. Nat Cell Biol 7: 1261-1266.
45. Brengues M, Teixeira D, Parker R (2005) Movement of eukaryotic mRNAs between polysomes and cytoplasmic processing bodies. Science 310: 486-489.

46. Filipowicz W, Bhattacharyya SN, Sonenberg N (2008) Mechanisms of post-transcriptional regulation by microRNAs: are the answers in sight? Nat Rev Genet 9: 102-114.

47. Pillai RS, Bhattacharyya SN, Artus CG, Zoller T, Cougot N, et al. (2005) Inhibition of translational initiation by Let-7 MicroRNA in human cells. Science 309: 1573-1576.

48. Humphreys DT, Westman BJ, Martin DI, Preiss T (2005) MicroRNAs control translation initiation by inhibiting eukaryotic initiation factor 4E/cap and poly(A) tail function. Proc Natl Acad Sci U S A 102: 16961-16966.

49. Kiriakidou M, Tan GS, Lamprinaki S, De Planell-Saguer M, Nelson PT, et al. (2007) An mRNA m7G cap binding-like motif within human Ago2 represses translation. Cell 129: 1141-1151.

50. Chendrimada TP, Gregory RI, Kumaraswamy E, Norman J, Cooch N, et al. (2005) TRBP recruits the Dicer complex to Ago2 for microRNA processing and gene silencing. Nature 436: 740-744.

51. Chendrimada TP, Finn KJ, Ji X, Baillat D, Gregory RI, et al. (2007) MicroRNA silencing through RISC recruitment of eIF6. Nature 447: 823-828.

52. Olsen PH, Ambros V (1999) The lin-4 regulatory RNA controls developmental timing in Caenorhabditis elegans by blocking LIN-14 protein synthesis after the initiation of translation. Dev Biol 216: 671-680.

53. Petersen CP, Bordeleau ME, Pelletier J, Sharp PA (2006) Short RNAs repress translation after initiation in mammalian cells. Mol Cell 21: 533-542.

54. Behm-Ansmant I, Rehwinkel J, Doerks T, Stark A, Bork P, et al. (2006) mRNA degradation by miRNAs and GW182 requires both CCR4:NOT deadenylase and DCP1:DCP2 decapping complexes. Genes Dev 20: 1885-1898.

55. Fabian MR, Mathonnet G, Sundermeier T, Mathys H, Zipprich JT, et al. (2009) Mammalian miRNA RISC recruits CAF1 and PABP to affect PABP-dependent deadenylation. Mol Cell 35: 868-880.
56. John B, Enright AJ, Aravin A, Tuschl T, Sander C, et al. (2004) Human MicroRNA targets. PLoS Biol 2: e363.
57. Krek A, Grun D, Poy MN, Wolf R, Rosenberg L, et al. (2005) Combinatorial microRNA target predictions. Nat Genet 37: 495-500.
58. Lewis BP, Burge CB, Bartel DP (2005) Conserved seed pairing, often flanked by adenosines, indicates that thousands of human genes are microRNA targets. Cell 120: 15-20.
59. Paraskevopoulou MD, Georgakilas G, Kostoulas N, Vlachos IS, Vergoulis T, et al. (2013) DIANA-microT web server v5.0: service integration into miRNA functional analysis workflows. Nucleic Acids Res 41: W169-173.
60. Kertesz M, Iovino N, Unnerstall U, Gaul U, Segal E (2007) The role of site accessibility in microRNA target recognition. Nat Genet 39: 1278-1284.
61. Loher P, Rigoutsos I (2012) Interactive exploration of RNA22 microRNA target predictions. Bioinformatics 28: 3322-3323.
62. Neilson JR, Sharp PA (2008) Small RNA regulators of gene expression. Cell 134: 899-902.
63. Croce CM (2009) Causes and consequences of microRNA dysregulation in cancer. Nat Rev Genet 10: 704-714.
64. Kong YW, Ferland-McCollough D, Jackson TJ, Bushell M (2012) microRNAs in cancer management. Lancet Oncol 13: e249-258.
65. Krol J, Loedige I, Filipowicz W (2010) The widespread regulation of microRNA biogenesis, function and decay. Nat Rev Genet 11: 597-610.

66. Tang X, Zhang Y, Tucker L, Ramratnam B (2010) Phosphorylation of the RNase III enzyme Drosha at Serine300 or Serine302 is required for its nuclear localization. Nucleic Acids Res 38: 6610-6619.
67. Tang X, Wen S, Zheng D, Tucker L, Cao L, et al. (2013) Acetylation of drosha on the N-terminus inhibits its degradation by ubiquitination. PLoS One 8: e72503.
68. Davis BN, Hilyard AC, Lagna G, Hata A (2008) SMAD proteins control DROSHA-mediated microRNA maturation. Nature 454: 56-61.
69. Ryan BM, Robles AI, Harris CC (2010) Genetic variation in microRNA networks: the implications for cancer research. Nat Rev Cancer 10: 389-402.
70. Heo I, Joo C, Cho J, Ha M, Han J, et al. (2008) Lin28 mediates the terminal uridylation of let-7 precursor MicroRNA. Mol Cell 32: 276-284.
71. Katoh T, Sakaguchi Y, Miyauchi K, Suzuki T, Kashiwabara S, et al. (2009) Selective stabilization of mammalian microRNAs by 3' adenylation mediated by the cytoplasmic poly(A) polymerase GLD-2. Genes Dev 23: 433-438.
72. Yang W, Chendrimada TP, Wang Q, Higuchi M, Seeburg PH, et al. (2006) Modulation of microRNA processing and expression through RNA editing by ADAR deaminases. Nat Struct Mol Biol 13: 13-21.
73. Xhemalce B, Robson SC, Kouzarides (2012) T Human RNA methyltransferase BCDIN3D regulates microRNA processing. Cell 151: 278-288.
74. Chatterjee S, Grosshans H (2009) Active turnover modulates mature microRNA activity in Caenorhabditis elegans. Nature 461: 546-549.
75. Bail S, Swerdel M, Liu H, Jiao X, Goff LA, et al. (2010) Differential regulation of microRNA stability. Rna 16: 1032-1039.
76. Das SK, Sokhi UK, Bhutia SK, Azab B, Su ZZ, et al. (2010) Human polynucleotide phosphorylase selectively and preferentially degrades

microRNA-221 in human melanoma cells. Proc Natl Acad Sci U S A 107: 11948-11953.

77. Ameres SL, Hung JH, Xu J, Weng Z, Zamore PD (2011) Target RNA-directed tailing and trimming purifies the sorting of endo-siRNAs between the two Drosophila Argonaute proteins. Rna 17: 54-63.
78. Rutnam ZJ, Yang BB (2012) The involvement of microRNAs in malignant transformation. Histol Histopathol 27: 1263-1270.
79. Calin GA, Croce CM (2006) MicroRNA signatures in human cancers. Nat Rev Cancer 6: 857-866.
80. Calin GA, Croce CM (2006) MicroRNA-cancer connection: the beginning of a new tale. Cancer Res 66: 7390-7394.
81. Gusev Y, Brackett DJ (2007) MicroRNA expression profiling in cancer from a bioinformatics prospective. Expert Rev Mol Diagn 7: 787-792.
82. Doleshal M, Magotra AA, Choudhury B, Cannon BD, Labourier E, et al. (2008) Evaluation and validation of total RNA extraction methods for microRNA expression analyses in formalin-fixed, paraffin-embedded tissues. J Mol Diagn 10: 203-211.
83. Raveche ES, Salerno E, Scaglione BJ, Manohar V, Abbasi F, et al. (2007) Abnormal microRNA-16 locus with synteny to human 13q14 linked to CLL in NZB mice. Blood 109: 5079-5086.
84. Hu Z, Chen J, Tian T, Zhou X, Gu H, et al. (2008) Genetic variants of miRNA sequences and non-small cell lung cancer survival. J Clin Invest 118: 2600-2608.
85. Ben Gacem R, Ben Abdelkrim O, Ziadi S, Ben Dhiab M, Trimeche M (2014) Methylation of miR-124a-1, miR-124a-2, and miR-124a-3 genes correlates with aggressive and advanced breast cancer disease. Tumour Biol 35: 4047-4056.
86. Kitagawa N, Ojima H, Shirakihara T, Shimizu H, Kokubu A, et al. (2013) Downregulation of the microRNA biogenesis components and its

association with poor prognosis in hepatocellular carcinoma. Cancer Sci 104: 543-551.

87. He L, He X, Lim LP, de Stanchina E, Xuan Z, et al. (2007) A microRNA component of the p53 tumour suppressor network. Nature 447: 1130-1134.

88. Chin LJ, Ratner E, Leng S, Zhai R, Nallur S, et al. (2008) A SNP in a let-7 microRNA complementary site in the KRAS 3' untranslated region increases non-small cell lung cancer risk. Cancer Res 68: 8535-8540.

89. Rothschild SI (2013) Epigenetic Therapy in Lung Cancer - Role of microRNAs. Front Oncol 3: 158.

90. Levin VA (2007) Are gliomas preventable? Recent Results Cancer Res 174: 205-215.

91. Nakada M, Nakada S, Demuth T, Tran NL, Hoelzinger DB, et al. (2007) Molecular targets of glioma invasion. Cell Mol Life Sci 64: 458-478.

92. Louis DN, Ohgaki H, Wiestler OD, Cavenee WK, Burger PC, et al. (2007) The 2007 WHO classification of tumours of the central nervous system. Acta Neuropathol 114: 97-109.

93. Haemmig S, Baumgartner U, Gluck A, Zbinden S, Tschan MP, et al. (2014) miR-125b controls apoptosis and temozolomide resistance by targeting TNFAIP3 and NKIRAS2 in glioblastomas. Cell Death Dis 5: e1279.

94. Henriksen M, Johnsen KB, Andersen HH, Pilgaard L, Duroux M (2014) MicroRNA Expression Signatures Determine Prognosis and Survival in Glioblastoma Multiforme-a Systematic Overview. Mol Neurobiol.

95. Hermansen SK, Kristensen BW (2013) MicroRNA biomarkers in glioblastoma. J Neurooncol 114: 13-23.

96. Nagasawa DT, Chow F, Yew A, Kim W, Cremer N, et al. (2012) Temozolomide and other potential agents for the treatment of glioblastoma multiforme. Neurosurg Clin N Am 23: 307-322, ix.

97. Sengupta S, Marrinan J, Frishman C, Sampath P (2012) Impact of temozolomide on immune response during malignant glioma chemotherapy. Clin Dev Immunol 2012: 831090.

98. Moller HG, Rasmussen AP, Andersen HH, Johnsen KB, Henriksen M, et al. (2013) A systematic review of microRNA in glioblastoma multiforme: micro-modulators in the mesenchymal mode of migration and invasion. Mol Neurobiol 47: 131-144.

99. Selcuklu SD, Donoghue MT, Spillane C (2009) miR-21 as a key regulator of oncogenic processes. Biochem Soc Trans 37: 918-925.

100. Chan JA, Krichevsky AM, Kosik KS (2005) MicroRNA-21 is an antiapoptotic factor in human glioblastoma cells. Cancer Res 65: 6029-6033.

101. Hermansen SK, Dahlrot RH, Nielsen BS, Hansen S, Kristensen BW (2013) MiR-21 expression in the tumor cell compartment holds unfavorable prognostic value in gliomas. J Neurooncol 111: 71-81.

102. Sasayama T, Nishihara M, Kondoh T, Hosoda K, Kohmura E (2009) MicroRNA-10b is overexpressed in malignant glioma and associated with tumor invasive factors, uPAR and RhoC. Int J Cancer 125: 1407-1413.

103. Gabriely G, Yi M, Narayan RS, Niers JM, Wurdinger T, et al. (2011) Human glioma growth is controlled by microRNA-10b. Cancer Res 71: 3563-3572.

104. Quintavalle C, Mangani D, Roscigno G, Romano G, Diaz-Lagares A, et al. (2013) MiR-221/222 target the DNA methyltransferase MGMT in glioma cells. PLoS One 8: e74466.

105. Zhang C, Kang C, You Y, Pu P, Yang W, et al. (2009) Co-suppression of miR-221/222 cluster suppresses human glioma cell growth by targeting p27kip1 in vitro and in vivo. Int J Oncol 34: 1653-1660.

106. Quintavalle C, Garofalo M, Zanca C, Romano G, Iaboni M, et al. (2012) miR-221/222 overexpession in human glioblastoma increases

invasiveness by targeting the protein phosphate PTPmu. Oncogene 31: 858-868.

107. Burgoyne AM, Phillips-Mason PJ, Burden-Gulley SM, Robinson S, Sloan AE, et al. (2009) Proteolytic cleavage of protein tyrosine phosphatase mu regulates glioblastoma cell migration. Cancer Res 69: 6960-6968.

108. Bo Y, Guo G, Yao W (2013) MiRNA-mediated tumor specific delivery of TRAIL reduced glioma growth. J Neurooncol 112: 27-37.

109. Godlewski J, Nowicki MO, Bronisz A, Williams S, Otsuki A, et al. (2008) Targeting of the Bmi-1 oncogene/stem cell renewal factor by microRNA-128 inhibits glioma proliferation and self-renewal. Cancer Res 68: 9125-9130.

110. Papagiannakopoulos T, Friedmann-Morvinski D, Neveu P, Dugas JC, Gill RM, et al. (2012) Pro-neural miR-128 is a glioma tumor suppressor that targets mitogenic kinases. Oncogene 31: 1884-1895.

111. Zhang Y, Chao T, Li R, Liu W, Chen Y, et al. (2009) MicroRNA-128 inhibits glioma cells proliferation by targeting transcription factor E2F3a. J Mol Med (Berl) 87: 43-51.

112. Wuchty S, Arjona D, Li A, Kotliarov Y, Walling J, et al. (2011) Prediction of Associations between microRNAs and Gene Expression in Glioma Biology. PLoS One 6: e14681.

113. Wang Y, Li Y, Sun J, Wang Q, Sun C, et al. (2013) Tumor-suppressive effects of miR-29c on gliomas. Neuroreport 24: 637-645.

114. Niu CS, Yang Y, Cheng CD (2013) MiR-134 regulates the proliferation and invasion of glioblastoma cells by reducing Nanog expression. Int J Oncol 42: 1533-1540.

115. Whitman M (1998) Smads and early developmental signaling by the TGFbeta superfamily. Genes Dev 12: 2445-2462.

116. Eling TE, Baek SJ, Shim M, Lee CH (2006) NSAID activated gene (NAG-1), a modulator of tumorigenesis. J Biochem Mol Biol 39: 649-655.

117. Bootcov MR, Bauskin AR, Valenzuela SM, Moore AG, Bansal M, et al. (1997) MIC-1, a novel macrophage inhibitory cytokine, is a divergent member of the TGF-beta superfamily. Proc Natl Acad Sci U S A 94: 11514-11519.

118. Kakehi Y, Segawa T, Wu XX, Kulkarni P, Dhir R, et al. (2004) Down-regulation of macrophage inhibitory cytokine-1/prostate derived factor in benign prostatic hyperplasia. Prostate 59: 351-356.

119. Tan M, Wang Y, Guan K, Sun Y (2000) PTGF-beta, a type beta transforming growth factor (TGF-beta) superfamily member, is a p53 target gene that inhibits tumor cell growth via TGF-beta signaling pathway. Proc Natl Acad Sci U S A 97: 109-114.

120. Hromas R, Hufford M, Sutton J, Xu D, Li Y, et al. (1997) PLAB, a novel placental bone morphogenetic protein. Biochim Biophys Acta 1354: 40-44.

121. Lindahl B The story of growth differentiation factor 15: another piece of the puzzle. Clin Chem 59: 1550-1552.

122. Strelau J, Sullivan A, Bottner M, Lingor P, Falkenstein E, et al. (2000) Growth/differentiation factor-15/macrophage inhibitory cytokine-1 is a novel trophic factor for midbrain dopaminergic neurons in vivo. J Neurosci 20: 8597-8603.

123. Mimeault M, Batra SK (2010) Divergent molecular mechanisms underlying the pleiotropic functions of macrophage inhibitory cytokine-1 in cancer. J Cell Physiol 224: 626-635.

124. Bauskin AR, Brown DA, Junankar S, Rasiah KK, Eggleton S, et al. (2005) The propeptide mediates formation of stromal stores of PROMIC-1: role in determining prostate cancer outcome. Cancer Res 65: 2330-2336.

125. Fairlie WD, Moore AG, Bauskin AR, Russell PK, Zhang HP, et al. (1999) MIC-1 is a novel TGF-beta superfamily cytokine associated with macrophage activation. J Leukoc Biol 65: 2-5.

126. Albertoni M, Shaw PH, Nozaki M, Godard S, Tenan M, et al. (2002) Anoxia induces macrophage inhibitory cytokine-1 (MIC-1) in glioblastoma cells independently of p53 and HIF-1. Oncogene 21: 4212-4219.

127. Osada H, Yoshitake Y, Ikeda T, Ishigaki Y, Takata T, et al. (2011) Ultraviolet B-induced expression of amphiregulin and growth differentiation factor 15 in human lens epithelial cells. Mol Vis 17: 159-169.

128. Schopfer DW, Ku IA, Regan M, Whooley MA (2014) Growth differentiation factor 15 and cardiovascular events in patients with stable ischemic heart disease (The Heart and Soul Study). Am Heart J 167: 186-192 e181.

129. Tsai VW, Macia L, Johnen H, Kuffner T, Manadhar R, et al. (2013) TGF-b superfamily cytokine MIC-1/GDF15 is a physiological appetite and body weight regulator. PLoS One 8: e55174.

130. Bauskin AR, Brown DA, Kuffner T, Johnen H, Luo XW, et al. (2006) Role of macrophage inhibitory cytokine-1 in tumorigenesis and diagnosis of cancer. Cancer Res 66: 4983-4986.

131. Baek SJ, Wilson LC, Lee CH, Eling TE (2002) Dual function of nonsteroidal anti-inflammatory drugs (NSAIDs): inhibition of cyclooxygenase and induction of NSAID-activated gene. J Pharmacol Exp Ther 301: 1126-1131.

132. Kim KS, Baek SJ, Flake GP, Loftin CD, Calvo BF, et al. (2002) Expression and regulation of nonsteroidal anti-inflammatory drug-activated gene (NAG-1) in human and mouse tissue. Gastroenterology 122: 1388-1398.

133. Brown DA, Ward RL, Buckhaults P, Liu T, Romans KE, et al. (2003) MIC-1 serum level and genotype: associations with progress and prognosis of colorectal carcinoma. Clin Cancer Res 9: 2642-2650.

134. Lee DH, Yang Y, Lee SJ, Kim KY, Koo TH, et al. (2003) Macrophage inhibitory cytokine-1 induces the invasiveness of gastric cancer cells by up-regulating the urokinase-type plasminogen activator system. Cancer Res 63: 4648-4655.

135. Bruzzese F, Hagglof C, Leone A, Sjoberg E, Roca MS, et al. (2014) Local and systemic protumorigenic effects of cancer-associated fibroblast-derived GDF15. Cancer Res 74: 3408-3417.

136. Brown DA, Hance KW, Rogers CJ, Sansbury LB, Albert PS, et al. (2012) Serum macrophage inhibitory cytokine-1 (MIC-1/GDF15): a potential screening tool for the prevention of colon cancer? Cancer Epidemiol Biomarkers Prev 21: 337-346.

137. Johnen H, Lin S, Kuffner T, Brown DA, Tsai VW, et al. (2007) Tumor-induced anorexia and weight loss are mediated by the TGF-beta superfamily cytokine MIC-1. Nat Med 13: 1333-1340.

138. Boyle GM, Pedley J, Martyn AC, Banducci KJ, Strutton GM, et al. (2009) Macrophage inhibitory cytokine-1 is overexpressed in malignant melanoma and is associated with tumorigenicity. J Invest Dermatol 129: 383-391.

139. Baek SJ, Eling TE (2006) Changes in gene expression contribute to cancer prevention by COX inhibitors. Prog Lipid Res 45: 1-16.

140. Shim M, Eling TE (2005) Protein kinase C-dependent regulation of NAG-1/placental bone morphogenic protein/MIC-1 expression in LNCaP prostate carcinoma cells. J Biol Chem 280: 18636-18642.

141. Frizzell KM, Gamble MJ, Berrocal JG, Zhang T, Krishnakumar R, et al. (2009) Global analysis of transcriptional regulation by poly(ADP-ribose) polymerase-1 and poly(ADP-ribose) glycohydrolase in MCF-7 human breast cancer cells. J Biol Chem 284: 33926-33938.

142. Krieg AJ, Rankin EB, Chan D, Razorenova O, Fernandez S, et al. (2010) Regulation of the histone demethylase JMJD1A by hypoxia-inducible factor 1 alpha enhances hypoxic gene expression and tumor growth. Mol Cell Biol 30: 344-353.

143. Yamaguchi K, Lee SH, Eling TE, Baek SJ (2004) Identification of nonsteroidal anti-inflammatory drug-activated gene (NAG-1) as a novel downstream target of phosphatidylinositol 3-kinase/AKT/GSK-3beta pathway. J Biol Chem 279: 49617-49623.

144. Feng H, Chen L, Wang Q, Shen B, Liu L, et al. (2013) Calumenin-15 facilitates filopodia formation by promoting TGF-beta superfamily cytokine GDF-15 transcription. Cell Death Dis 4: e870.

145. Li A, Walling J, Ahn S, Kotliarov Y, Su Q, et al. (2009) Unsupervised analysis of transcriptomic profiles reveals six glioma subtypes. Cancer Res 69: 2091-2099.

146. Shnaper S, Desbaillets I, Brown DA, Murat A, Migliavacca E, et al. (2009) Elevated levels of MIC-1/GDF15 in the cerebrospinal fluid of patients are associated with glioblastoma and worse outcome. Int J Cancer 125: 2624-2630.

147. Wang X, Baek SJ, Eling T (2011) COX inhibitors directly alter gene expression: role in cancer prevention? Cancer Metastasis Rev 30: 641-657.

148. Jeansonne D, Pacifici M, Lassak A, Reiss K, Russo G, et al. (2013) Differential Effects of MicroRNAs on Glioblastoma Growth and Migration. Genes (Basel) 4: 46-64.

149. Kim JM, Kosak JP, Kim JK, Kissling G, Germolec DR, et al. (2013) NAG-1/GDF15 transgenic mouse has less white adipose tissue and a reduced inflammatory response. Mediators Inflamm 2013: 641851.

150. Yoshioka H, Kamitani H, Watanabe T, Eling TE (2008) Nonsteroidal anti-inflammatory drug-activated gene (NAG-1/GDF15) expression is

increased by the histone deacetylase inhibitor trichostatin A. J Biol Chem 283: 33129-33137.

151. Desvergne B, Wahli W (1999) Peroxisome proliferator-activated receptors: nuclear control of metabolism. Endocr Rev 20: 649-688.

152. Urbanska K, Pannizzo P, Grabacka M, Croul S, Del Valle L, et al. (2008) Activation of PPARalpha inhibits IGF-I-mediated growth and survival responses in medulloblastoma cell lines. Int J Cancer 123: 1015-1024.

153. Elijah IE, Borsheim E, Maybauer DM, Finnerty CC, Herndon DN, et al. (2012) Role of the PPAR-alpha agonist fenofibrate in severe pediatric burn. Burns 38: 481-486.

154. Grabacka M, Plonka PM, Urbanska K, Reiss K (2006) Peroxisome proliferator-activated receptor alpha activation decreases metastatic potential of melanoma cells in vitro via down-regulation of Akt. Clin Cancer Res 12: 3028-3036.

155. Issemann I, Green S (1990) Activation of a member of the steroid hormone receptor superfamily by peroxisome proliferators. Nature 347: 645-650.

156. Willson TM, Brown PJ, Sternbach DD, Henke BR (2000) The PPARs: from orphan receptors to drug discovery. J Med Chem 43: 527-550.

157. Schupp M, Lazar MA (2010) Endogenous ligands for nuclear receptors: digging deeper. J Biol Chem 285: 40409-40415.

158. Peters JM, Shah YM, Gonzalez FJ (2012) The role of peroxisome proliferator-activated receptors in carcinogenesis and chemoprevention. Nat Rev Cancer 12: 181-195.

159. Panigrahy D, Kaipainen A, Huang S, Butterfield CE, Barnes CM, et al. (2008) PPARalpha agonist fenofibrate suppresses tumor growth through direct and indirect angiogenesis inhibition. Proc Natl Acad Sci U S A 105: 985-990.

160. Murad H, Collet P, Huin-Schohn C, Al-Makdissy N, Kerjan G, et al. (2006) Effects of PPAR and RXR ligands in semaphorin 6B gene expression of human MCF-7 breast cancer cells. Int J Oncol 28: 977-984.

161. Zak Z, Gelebart P, Lai R (2010) Fenofibrate induces effective apoptosis in mantle cell lymphoma by inhibiting the TNFalpha/NF-kappaB signaling axis. Leukemia 24: 1476-1486.

162. Mantovani A, Allavena P, Sica A, Balkwill F (2008) Cancer-related inflammation. Nature 454: 436-444.

163. Koppenol WH, Bounds PL, Dang CV (2011) Otto Warburg's contributions to current concepts of cancer metabolism. Nat Rev Cancer 11: 325-337.

164. Aoyama T, Peters JM, Iritani N, Nakajima T, Furihata K, et al. (1998) Altered constitutive expression of fatty acid-metabolizing enzymes in mice lacking the peroxisome proliferator-activated receptor alpha (PPARalpha). J Biol Chem 273: 5678-5684.

165. Kersten S, Mandard S, Escher P, Gonzalez FJ, Tafuri S, et al. (2001) The peroxisome proliferator-activated receptor alpha regulates amino acid metabolism. Faseb J 15: 1971-1978.

166. Wolf A, Agnihotri S, Guha A (2010) Targeting metabolic remodeling in glioblastoma multiforme. Oncotarget 1: 552-562.

167. Strakova N, Ehrmann J, Bartos J, Malikova J, Dolezel J, et al. (2005) Peroxisome proliferator-activated receptors (PPAR) agonists affect cell viability, apoptosis and expression of cell cycle related proteins in cell lines of glial brain tumors. Neoplasma 52: 126-136.

168. Saidi SA, Holland CM, Charnock-Jones DS, Smith SK (2006) In vitro and in vivo effects of the PPAR-alpha agonists fenofibrate and retinoic acid in endometrial cancer. Mol Cancer 5: 13.

169. Araki H, Tamada Y, Imoto S, Dunmore B, Sanders D, et al. (2009) Analysis of PPARalpha-dependent and PPARalpha-independent

transcript regulation following fenofibrate treatment of human endothelial cells. Angiogenesis 12: 221-229.

170. Nadanaciva S, Dykens JA, Bernal A, Capaldi RA, Will Y (2007) Mitochondrial impairment by PPAR agonists and statins identified via immunocaptured OXPHOS complex activities and respiration. Toxicol Appl Pharmacol 223: 277-287.

171. Wybieralska E, Szpak K, Gorecki A, Bonarek P, Miekus K, et al. (2011) Fenofibrate attenuates contact-stimulated cell motility and gap junctional coupling in DU-145 human prostate cancer cell populations. Oncol Rep 26: 447-453.

172. Wilk A, Urbanska K, Grabacka M, Mullinax J, Marcinkiewicz C, et al. (2012) Fenofibrate-induced nuclear translocation of FoxO3A triggers Bim-mediated apoptosis in glioblastoma cells in vitro. Cell Cycle 11: 2660-2671.

173. Golas MM, Sander B, Will CL, Luhrmann R, Stark H (2003) Molecular architecture of the multiprotein splicing factor SF3b. Science 300: 980-984.

174. Kramer A (1996) The structure and function of proteins involved in mammalian pre-mRNA splicing. Annu Rev Biochem 65: 367-409.

175. Champion-Arnaud P, Reed R (1994) The prespliceosome components SAP 49 and SAP 145 interact in a complex implicated in tethering U2 snRNP to the branch site. Genes Dev 8: 1974-1983.

176. Terada Y, Yasuda Y (2006) Human immunodeficiency virus type 1 Vpr induces G2 checkpoint activation by interacting with the splicing factor SAP145. Mol Cell Biol 26: 8149-8158.

177. Orr SJ, Boutz DR, Wang R, Chronis C, Lea NC, et al. (2012) Proteomic and protein interaction network analysis of human T lymphocytes during cell-cycle entry. Mol Syst Biol 8: 573.

178. Souchet M, Portales-Casamar E, Mazurais D, Schmidt S, Leger I, et al. (2002) Human p63RhoGEF, a novel RhoA-specific guanine

nucleotide exchange factor, is localized in cardiac sarcomere. J Cell Sci 115: 629-640.

179. Cerione RA, Zheng Y (1996) The Dbl family of oncogenes. Curr Opin Cell Biol 8: 216-222.

180. Rojas RJ, Yohe ME, Gershburg S, Kawano T, Kozasa T, et al. (2007) Galphaq directly activates p63RhoGEF and Trio via a conserved extension of the Dbl homology-associated pleckstrin homology domain. J Biol Chem 282: 29201-29210.

181. Lutz S, Freichel-Blomquist A, Rumenapp U, Schmidt M, Jakobs KH, et al. (2004) p63RhoGEF and GEFT are Rho-specific guanine nucleotide exchange factors encoded by the same gene. Naunyn Schmiedebergs Arch Pharmacol 369: 540-546.

182. Goedhart J, van Unen J, Adjobo-Hermans MJ, Gadella TW, Jr. (2013) Signaling efficiency of Galphaq through its effectors p63RhoGEF and GEFT depends on their subcellular location. Sci Rep 3: 2284.

183. Hayashi A, Hiatari R, Tsuji T, Ohashi K, Mizuno K (2013) p63RhoGEF-mediated formation of a single polarized lamellipodium is required for chemotactic migration in breast carcinoma cells. FEBS Lett 587: 698-705.

184. Curtale G, Mirolo M, Renzi TA, Rossato M, Bazzoni F, et al. (2013) Negative regulation of Toll-like receptor 4 signaling by IL-10-dependent microRNA-146b. Proc Natl Acad Sci U S A 110: 11499-11504.

185. Stark MS, Tyagi S, Nancarrow DJ, Boyle GM, Cook AL, et al. (2010) Characterization of the Melanoma miRNAome by Deep Sequencing. PLoS One 5: e9685.

186. Sivadas VP, George NA, Kattoor J, Kannan S (2013) Novel mutations and expression alterations in SMAD3/TGFBR2 genes in oral carcinoma correlate with poor prognosis. Genes Chromosomes Cancer 52: 1042-1052.

187. Okamura K, Hagen JW, Duan H, Tyler DM, Lai EC (2007) The mirtron pathway generates microRNA-class regulatory RNAs in Drosophila. Cell 130: 89-100.

188. DeGregori J, Kowalik T, Nevins JR (1995) Cellular targets for activation by the E2F1 transcription factor include DNA synthesis- and G1/S-regulatory genes. Mol Cell Biol 15: 4215-4224.

189. Matsumura I, Tanaka H, Kanakura Y (2003) E2F1 and c-Myc in cell growth and death. Cell Cycle 2: 333-338.

LIST OF PUBLICATIONS

Jeansonne D*, De Luca M*, Marrero L, Lassak A, Pacifici M, Wyczechowska D, Wilk A, Reiss K and Peruzzi F. Anti-Tumoral Effects of miR-3189-3p in Glioblastoma. * Authors contributed equally. Manuscript submitted for publication to the Journal of Biological Chemistry.

Masieri S, Trabattoni D, Incorvaia C, De Luca MC, Dell'albani I, Leo G, Frati F. 2014. *A role for Waldeyer's ring in immunological response to allergens*. Curr Med Res Opin; 30 (2): 203 - 205.

Biasin M., De Luca M., Gnudi F., Clerici M. 2013. *The genetic basis of resistance to HIV infection and disease progression*. Expert Review of Clinical Immunology; 9(4):319-34.

Biasin M., Sironi M., Saulle I., De Luca M., La Rosa F., Cagliani R., Forni D., Agliardi C., Lo Caputo S., Mazzotta F., Trabattoni D., Macias J., Pineda J. A., Caruz A., Clerici M. 2013. *Endoplasmic reticulum aminopeptidase 2 (ERAP2) haplotypes play a role in modulating susceptibility to HIV infection*. AIDS.

Rossato M., Curtale G., Tamassia N., Castellucci M., Mori L., Gasperini S., Mariotti B., De Luca M., Mirolo M., Cassatella MA, Locati M., Bazzoni F. 2012. *IL-10-induced microRNA-187 negatively regulates TNF-α, IL-6, and IL-12p40 production in TLR4-stimulated monocytes.* Proc Natl Acad Sci USA; 109(45):E3101-10.

Sironi M., Biasin M., Forni D., Cagliani R., De Luca M., Saulle I., Lo Caputo S., Mazzotta F., Macias J., Pineda J. A., Caruz A., Clerici M. 2012. *Genetic variability at the TREX1 locus is not associated with natural resistance to HIV-1 infection*. AIDS; 26(11):1443-5.

Sironi M., Biasin M., Cagliani R., Forni D., De Luca M., Saulle I., Lo Caputo S., Mazzotta F., Macìas J., Pineda J. A., Caruz A., Clerici M. 2011. *A Common Polymorphism in TLR3 Confers Natural Resistance to HIV-1 Infection*. The Journal of Immunology; 188(2):818-23.

ACKNOWLEDGMENTS

Vorrei innanzitutto ringraziare la Prof. Daria Trabattoni e il Prof. Mario Clerici per avermi supportato durante l'attivita' di ricerca in questi tre anni di Dottorato e per avermi dato l'opportunita' di svolgere parte di essa all'estero.

Un grazie di cuore va alla Prof. Francesca Peruzzi, alla sua disponibilita' per avermi accolto nel suo laboratorio "in quel di New Orleans" e avermi insegnato il rigore scientifico e l'approccio sperimentale.

Grazie a tutti i miei colleghi del Louisiana Cancer Research Center, non basterebbe questa pagina per dirvi quanto siete stati carini e accoglienti nei miei confronti cercando di aiutarmi qualunque volta ne avessi bisogno e facendomi sentire un po' meno lontano da casa… Grazie ad Adam, Ania, Jimena, Adriana, Amanda, Michael, Matthew, Kris, Louis, Jovanny, Claudia, Maria Elena, Li, Dorotha e Dulfary.

Un ringraziamento speciale ai miei due compagni di viaggio e di avventure Duane e Ferdous, a tutto quello che mi avete insegnato… grazie per avermi sempre aiutato in ogni situazione e condiviso con me gioie e dolori di ogni esperimento!

Grazie a tutte le colleghe e amiche del laboratorio di Immunologia: Mara, Fede, Irma, Micaela, Sara, Veronica e Angela. Con voi mi sono fatta le migliori risate e… serate in laboratorio!

Grazie al mio mitico gruppo della "Big Easy": Silvia, Virginia, Erminia e Salome'. Dal laboratorio, alla spesa, alle gite fuori porta… solo voi, con la vostra stravaganza e il vostro esserci sempre e comunque in qualsiasi circostanza, avete reso questa esperienza speciale ed indimenticabile.

Grazie a tutti coloro che, seppur lontani, mi hanno fatto sentire la loro vicinanza sempre!

Ovviamente tutto cio' non sarebbe stato possibile senza il supporto della mia famiglia! Grazie a mamma e papa', a Dani e a Claudia e alla Nonna Maria… solo voi sapete darmi il coraggio, la forza di andare avanti e di lottare sempre per quello in cui credo!

Infine grazie a tutte le persone che, seppur con una presenza "fugace", hanno in qualche modo contribuito a farmi crescere sia dal punto di vista professionale che personale… a volte basta solo una parola, una frase detta nel modo giusto e al momento giusto per evitare di scoraggiarsi e continuare a credere nei propri sogni!